# DESIGN OF A PLASMA ABATEMENT SYSTEM FOR PERFLUORONATED COMPOUNDS

A Thesis

by

MATTHEW ROBERT BUTLER

Submitted to the Office of Graduate Studies of
Texas A&M University
in partial fulfillment of the requirements for the degree of

MASTER OF SCIENCE

May 2011

Major Subject: Mechanical Engineering

# DESIGN OF A PLASMA ABATEMENT SYSTEM FOR PERFLUORONATED COMPOUNDS

A Thesis

by

MATTHEW ROBERT BUTLER

Submitted to the Office of Graduate Studies of
Texas A&M University
in partial fulfillment of the requirements for the degree of

MASTER OF SCIENCE

Approved by:

| | |
|---|---|
| Chair of Committee, | Dennis O'Neal |
| Committee Members, | Andrew Duggleby |
| | Michael Pate |
| | Brock Faulkner |
| Head of Department, | Dennis O'Neal |

May 2011

Major Subject: Mechanical Engineering

# ABSTRACT

Design of a Plasma Abatement System for Perfluoronated Compounds. (May 2011)

Matthew Robert Butler, B.S., New Mexico State University

Chair of Advisory Committee: Dr. Dennis O'Neal

The plasma abatement system co-developed by R*f* Environmental, Inc. and Texas A&M University has been effective at destroying the global warming gases $CF_4$ and $C_4F_8$. The destruction of greenhouse gases, specifically perfluorocompounds, hydrofluorocompounds, chlorofluorocompounds (PFCs, HFCs, CFCs) and $SF_6$, is paramount to significantly affecting atmospheric pollution. The premise of this study was to examine the design of the plasma abatement system for Global Warming Gases (GWGs) and its abatement potential for these gases.

The first goal was to reduce the cost of ownership by examining the cooling system. The cost of an air cooling design was $1400/yr. The intent was to reduce the amount of air used or use a different medium that would produce the same amount of heat transfer. A liquid cooling system design had a cost of only $150/yr. A $C_4F_8$ abatement experiment was run on the liquid cooling design. The abatement process resulted in a destruction removal efficiency (DRE) of $C_4F_8$ of 97.5%. A lower operational cost unit was developed, but the operational performance was less than previous investigations.

The second goal was to simulate the semiconductor radio frequency etching process and abate the output gases of the $C_4F_8$ and $SiO_2$ reaction. The outcomes of this

experiment included a microwave simulation of the radio frequency etching reaction and an abatement that resulted in a 99.98 ±.05% DRE for $C_4F_8$ with no formation of any other CFC gases.

The third goal was to simulate the etching process and abate the output gas, $CF_4$ using $H_2O$ vapor as the additive gas. The outcomes of this experiment included a microwave simulation of the radio frequency etching reaction and an abatement that resulted in a 99.96 ±.05% DRE for $CF_4$ with no formation of any other CFC gases.

A low cost of ownership and effective abatement levels will make this system viable for commercial use. The latest data shows the amount of PFC emissions from the semiconductor industry was 3.6 Tg $CO_2$ Eq. The use of this or a similar abatement technology will have a significant impact on reducing environmental pollution.

# DEDICATION

To my parents, who have always encouraged and supported me

To my lovely wife Emily, without whom, I would not have been able to finish

## ACKNOWLEDGMENTS

The progression of this research would not have been possible without the financial support of the Environmental Protection Agency, SEMATECH, The Center for Atmospheric Chemistry and the Environment at Texas A&M University, and R*f* Environmental, Inc.

I would also like to thank Bill Wofford, Michelle Frantzen and Blake McElmurry. I would like to especially thank my advisor Dr. John Bevan who directed this effort and supported my research these many years. Their guidance and instruction was crucial to my understanding of chemistry. I was able to produce this research because of their past achievements.

# TABLE OF CONTENTS

Page

# LIST OF TABLES

Page

## LIST OF FIGURES

Page

Page

## NOMENCLATURE

| | |
|---|---|
| CFC | Chlorofluorocompound |
| COO | Cost of Ownership |
| CVD | Chemical Vapor Deposition |
| DRE | Destruction Removal Efficiency |
| EPA | Environmental Protection Agency |
| FTIR | Fourier Transform Infra-Red |
| GHG | Green House Gas |
| GWP | Global Warming Potential |
| HFC | Hydrofluorocompound |
| IPCC | Intergovernmental Panel on Climate Change |
| MMTCE | Million Metric Tons of Carbon Equivalent |
| PAS | Plasma Abatement System |
| PFC | Perfluorocompound |
| Sccm | Standard Cubic Centimeters per Minute |
| SIA | Semiconductor Industry Association |
| SWP | Surface Wave Plasma |
| WSC | World Semiconductor Council |

# 1. INTRODUCTION

The plasma abatement system (PAS) co-developed by R*f* Environmental, Inc. and Texas A&M University was designed to destroy harmful gaseous compounds. Several studies on this system were published on the destruction of those gases, including but not limited to $CHF_3$, $CF_4$ and $C_4F_8$ [1-4]. In its 3rd generation of design, the system has shown its robustness in producing high destruction removal efficiencies (DRE) from semiconductor reactant gases. Experimental studies by Frantzen[1] and Wofford[2] have shown that the PAS can abate the un-reacted compounds of $CF_4$ and $C_4F_8$. This thesis will show the effectiveness of this system to abate post reacted $SiO_2$ waste gases from the semiconductor etching process. It will also lower the cost of ownership (COO) by changing the systems cooling design.

The destruction of greenhouse gases (GHG), specifically perfluorocompounds, hydrofluorocompounds, chlorofluorocompounds (PFCs, HFCs, CFCs) and $SF_6$, is paramount to significantly affecting atmospheric pollution. The IPCC (Intergovernmental Panel on Climate Change) in its 4th Assessment Report (AR4) predicted that ecosystems, food supply, health, coasts and waters would be adversely affected, and have a high likelihood of happening if greenhouse gas emissions are not

This thesis follows the style of *Journal of Hazardous Materials.*

reduced[5]. A significant finding of the AR4 was that carbon dioxide's ($CO_2$) "annual emissions have grown between 1970 and 2004 by about 80%, from 21 to 38 gigatonnes (Gt), and represented 77% of total anthropogenic GHG emissions in 2004". The possibility of these damages necessitates the reduction and elimination of these compounds before they enter the atmosphere.

The IPCC stated in its Second Assessment Report (SAR) that, "Human activities are changing the atmospheric concentrations and distributions of greenhouse gases and aerosols. These changes can produce a phenomena called "radiative forcing" by changing either the reflection or absorption of solar radiation, or the emission and absorption of terrestrial radiation."[6] Radiative forcing is a measure of the importance of a climate change mechanism and is defined as the change in the net energy balance (expressed in $W*m^2$) of the Earth-atmosphere system hypothesis is that a semiconductor radio frequency etching reaction of $CF_4$ can be simulated using a microwave power source and the products from that reaction can be abated using $H_2O$ vapor as the additive gas to greater than 99% DRE.. Thus, it is the difference between incoming and outgoing radiation from the earth's climate system. The different components of the earth's climate system and some of their interactions are shown in *Figure* 1 below.

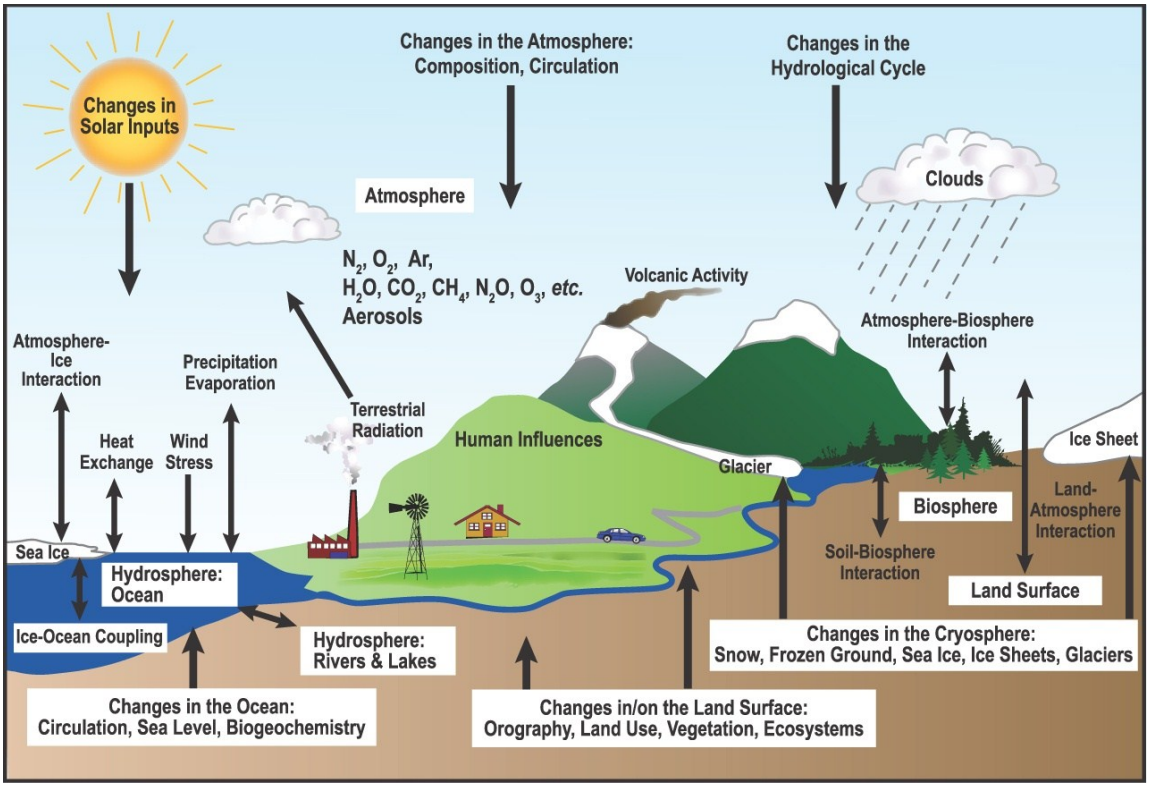


*Figure* 1. Schematic View of the Components of the Climate System, Their Processes and Interactions. [7]

Human industry is having an impact on the local environment through industry processes, electricity and fuel combustion, where greenhouse emissions have risen by 17.2% from 1990 to 2007[8]. This influence has been hypothesized to attribute to global climate change as well.[9]. These effects have been documented in the temperature of the earth's surface where the mean surface temperature has risen by 0.74 ± 0.18°C over the last 100 years. The rate has increased over shorter spans of time to 0.128 ± 0.026°C and 0.177°C ± 0.052°C for 50 and 25 years respectively.

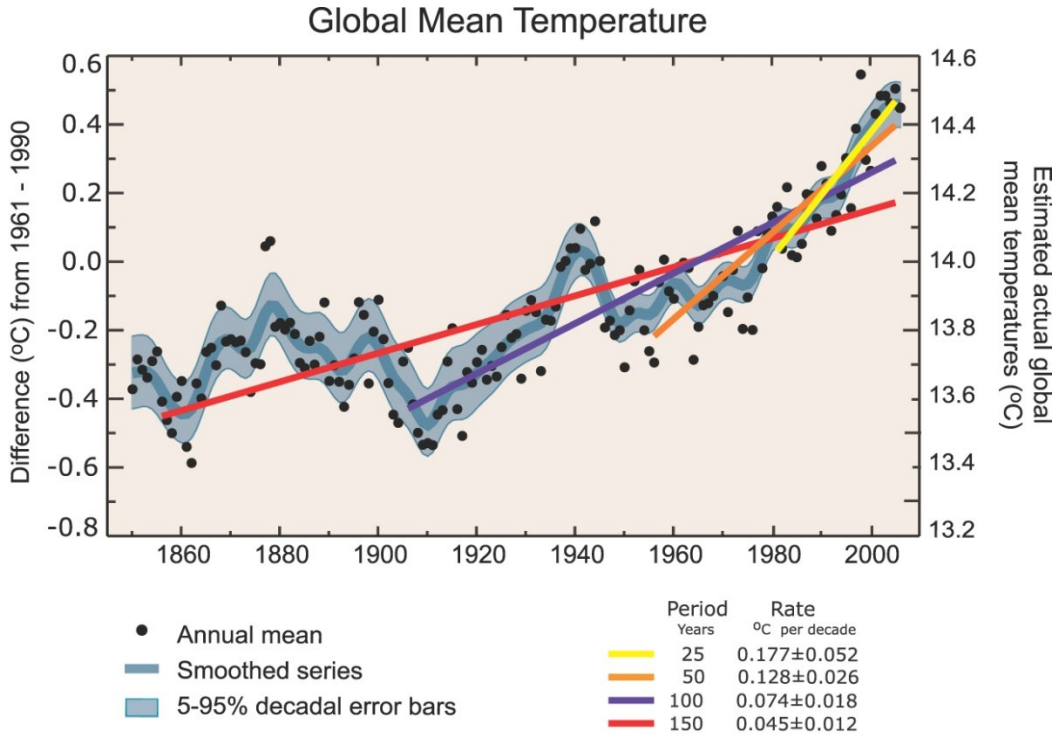


*Figure* 2. Annual Global Mean Observed Temperatures with Simple Fits to the Data.[9]

The importance of industrial growth has often preceded the need for protecting the earth, especially when the danger is theoretical. Given that there is now scientific evidence (as shown in *Figure* 2) concluding warming trends and GHG build-up[9], the industries are now faced with decisions on how to lessen the upsurge in emissions. Specifically, the semiconductor industry is an important industry of focus due to its use of PFCs (perfluorocompounds) in its fabrication facilities.

On a global scale, the World Semiconductor Council (WSC), an international body consisting of semiconductor manufacturers in China, Europe, Japan, Korea and the United States has agreed upon a voluntary goal to reduce PFC emissions by ten percent by the year 2010, with respect to a baseline emission[10]. The baselines are 1995, 1997,

or 1998 emissions depending on when the manufacturer joined the WSC[11]. Emissions from United States companies were 4.9, 6.3 and 7.1 Tg-$CO_2$-eq/yr respectively, other member emissions were unavailable. The emissions from semiconductor producing countries are listed in million metric tons of carbon equivalent in Table 1. It was initially estimated that semiconductor 200mm fabs would need to reduce absolute emissions by 90% for etch and 95% for CVD (chemical vapor deposition) processing relative to 1995 levels.[12] *Figure* 3 shows the original projected emission levels with no reduction strategies implemented. It also shows the actual emission values since 1995.

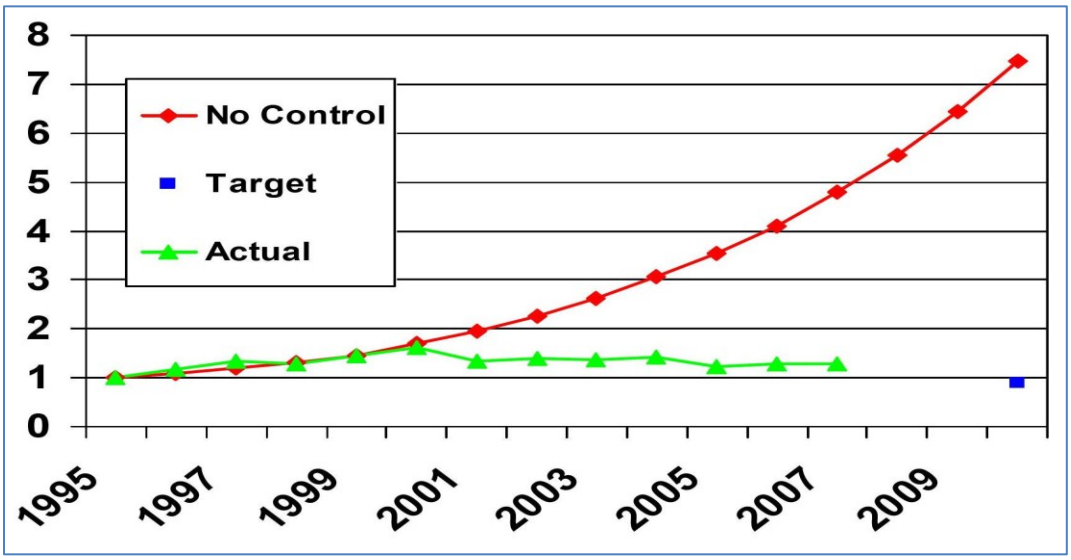


*Figure* 3. WSC PFC Emission Reduction Announcement and Data[10]

Table 1. PFC Emissions Estimates by Region [13]

| Region | 1995 MMTCE | 2000 MMTCE | 2005 MMTCE |
|---|---|---|---|
| **WSC** | 6.34 | 9.46 | 13.63 |
| US | 1.48 | 2.26 | 3.39 |
| Japan | 3.62 | 4.18 | 4.46 |
| Europe | 0.55 | 1.18 | 1.19 |
| Taiwan | 0.29 | 1.05 | 3.06 |
| Korea | 0.41 | 0.79 | 1.53 |
| **Non-WSC** | 0.78 | 1.25 | 3.08 |
| China | 0.1 | 0.2 | 0.99 |
| Singapore | 0.18 | 0.21 | 0.54 |
| Malaysia | 0 | 0 | 0.14 |
| Rest Of World | 0.49 | 0.84 | 1.4 |
| **Total** | **7.12** | **10.71** | **16.71** |

The WSC members have actively shared non-competitive information on these abatement technologies. Since the start of the program, companies have devoted considerable resources to meeting their voluntary reduction goals. They have implemented several strategies to accomplish this including:

- Optimization of the current technology
- Alternative chemistry
- Recycle / Recovery
- Abatement/Destruction

A more detailed description of the different technologies and strategies is shown below in *Figure* 4.

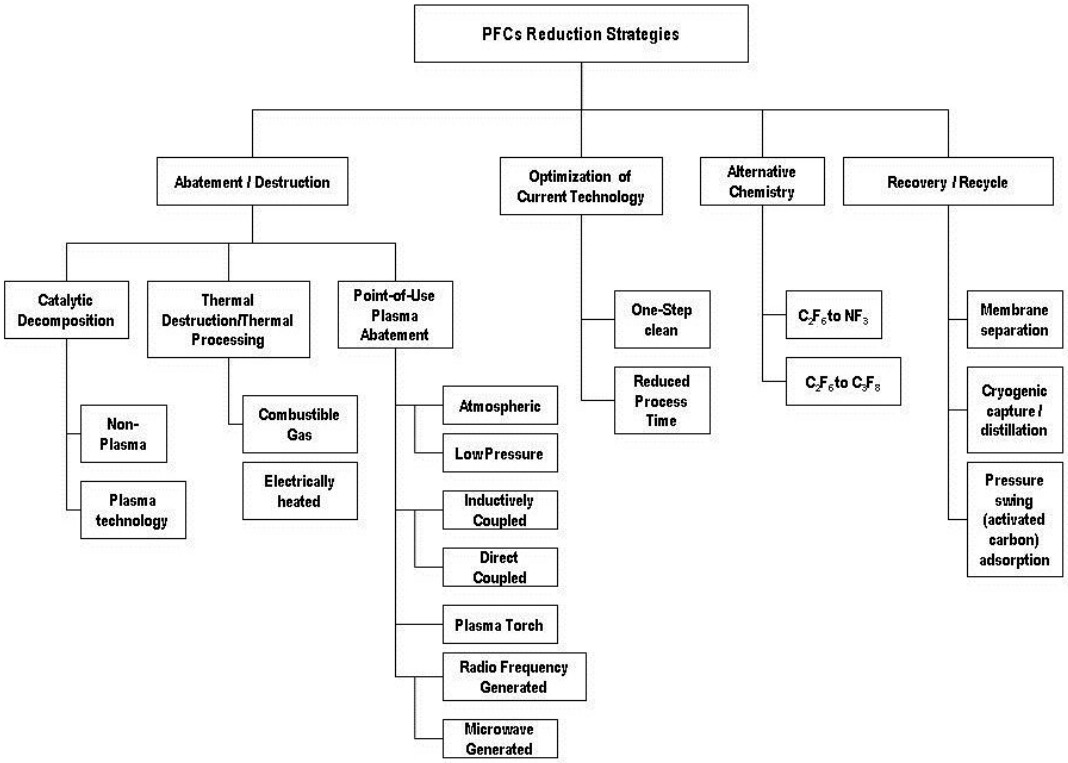


*Figure* 4. PFC Reduction Strategies

Process optimization strategies were implemented that reduced PFC emissions and shortened process times in the industry. This improved tool throughput and resulted in less tool erosion over time.[14] Another optimization process was changing from a two-step chamber clean to a one-step chamber clean. Through varying pressures, a reduction of gas flow of 33% and cycle time of 25% was realized. This produced a possible reduction of 50% of PFC gas usage.[14] Streif and team were able to reduce process gases usage between 50% and 70%, for a savings of $215,000 per year is gases alone.[15]

Alternative chemistry efforts have been aimed at the CVD chamber cleaning process. Changing gases from $C_2F_6$ to $NF_3$ for the chamber clean was implemented.[16] While the GWP was higher, as shown in the table on page 13, it is much more efficient, so it required less gas for the same results. Less gas was needed to perform the same function and the gas reacted more fully. The in situ $NF_3$ Clean Technology from Novellus and the $NF_3$ Remote Clean™ Technology from Applied Materials showed a reduction in PFC emissions of 90% and 95% respectively.[16] Motorola concluded that substituting $C_2F_6$ to $C_3F_8$, the $C_3F_8$ process: used less gas (24% less etch gas and 3 1 % less oxygen by mass), had a similar process duration to the standard $C_2F_6$ clean process, and reduced net PFC emissions measured as MMTCE by approximately 50%.[17]

Recycle and recovery technologies separate unused or unprocessed gases to be used for further processing. The adsorption process is a common method for the capture and recovery of organic vapors/gases which is based on the interaction between adsorbate and adsorbent. It has been hypothesized that semiconductor radio frequency etching reaction of $CF_4$ can be simulated using a microwave power source and the products from that reaction can be abated using $H_2O$ vapor as the additive gas to greater than 99% DRE. Other methods include cryogenic concentration and distillation and membrane separation.[18] Technologies in 2001 were reported to be 90% efficient for $C_2F_6$, $CF_4$, $SF_6$, and $C_3F_8$, and 50-60% for $CHF_3$ and $NF_3$[16]. There was significant pretreatment necessary to remove materials undesirable for the separation technology. The costs for destroying fluorocarbon gases was estimated at $3/kg and the cost for

recycling/recovery was significantly more[16, 19]. The high cost of this technology did not make it economically feasible for the industry to adopt.

Abatement technologies have been divided into Point-of-Use Plasma Abatement, Thermal Destruction/Thermal Processing Units and Catalytic Decomposition Systems. First approach technologies used thermal oxidation, but were found to be non-viable for the stable $CF_4$ molecule.[20] Point-of-use plasma abatement systems use a small plasma source in the fore-line of the etch tool or gas line. It disassociates the PFC molecules with additive reactants ($H_2$, $O_2$, $H_2O$ or $CH_4$) in order to produce lower level molecular components.[16, 21] The products are then removed with wet scrubbers. The research in this thesis focuses on the Fore-line Plasma method because of its ability to destroy $CF_4$ and it's relatively low cost per unit. Vartanian and Wofford worked with Motorola's facilities to test a foreline plasma abatement system that reduced $CF_4$ and $CHF_3$ emissions by 99% for flow rates of less than 100 $cm^3$/min [22]. Radiou was able to produce a $CF_4$ DRE of 95% with a flow rate of 25 l/min.[23]

Thermal destruction/thermal processing units (TPUs) require a combustion fuel to destroy the PFC. TPUs can be used on the CVD process as well as the etch process and do not affect the manufacturing process.[14] In addition to requiring large amounts of fuel, large amounts of waste water are generated requiring treatment as an industrial waste. [16]

Catalytic Decomposition Systems use a solid reactant to react with the fluorinated compounds. Catalytic decomposition systems also utilize non-thermal plasma technology to disassociate the compounds. Reactants like $Ca(OH)_2$ /CaO produce

$CaF_2$ as a product which is nonhazardous and does not require a water scrubber.[14, 24] The removal efficiency for this process has been shown to be greater than 99%. Further details of these technologies will be described later in the section.

Locally, PFC emissions in the United States have been tracked by the Environmental Protection Agency (EPA) since 1990. *Figure 5* shows the trend of PFC emissions from the semiconductor industry. As an industry, the manufacture of silicon wafers produced approximately 6 Tg of emissions in 1995. The output predictions at that time showed an upward trend based upon the expected industry's growth, not its actual growth. Based on these predictions an effort to maintain the levels of emissions was put into place. This goal only halted the growth of the level of pollution. Moreover, this focus by the EPA has led the Semiconductor Industry Association (SIA) to commit to a self-regulated 10 percent reduction based on the 1995 emission rate. The SIA's members include over 70 companies and account for 90% of the production in the United States.[25] Although not all semiconductor companies in the United States are members of the SIA, the EPA estimates emissions from all of the semiconductor manufacturers. Emission data is reported through the EPA's PFC Reduction/Climate Partnership and its PFC Emissions Vintage Model (PEVM).[8]

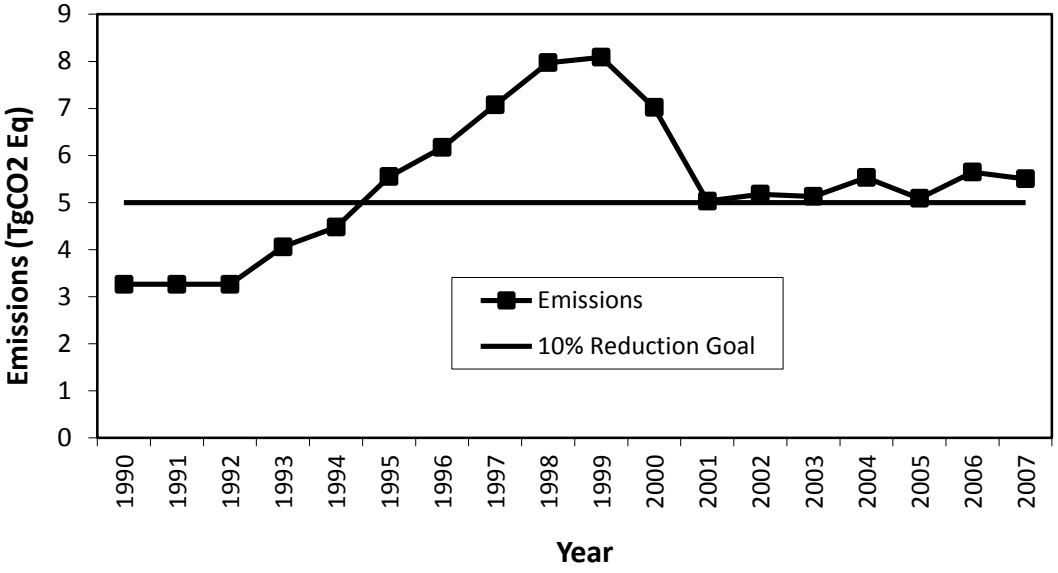


*Figure* 5. United States Semiconductor PFC Emissions, 2009 Report[8, 26]

The EPA has drawn attention to a particular subset of gases that augment the effects of $CO_2$. $CO_2$ is a natural greenhouse gas that traps heat energy on the surface of the earth. Distinctively, the industrial production of $CO_2$ and other aerosols when combined in the atmosphere alter the balance of the effects of naturally produced $CO_2$. *Figure* 6 shows the concentrations of $CO_2$, $CH_4$ and $N_2O$ over the last 2000 years. The amount of $CO_2$ found in ice core data shows a dramatic increase in concentration in the last 200 years.

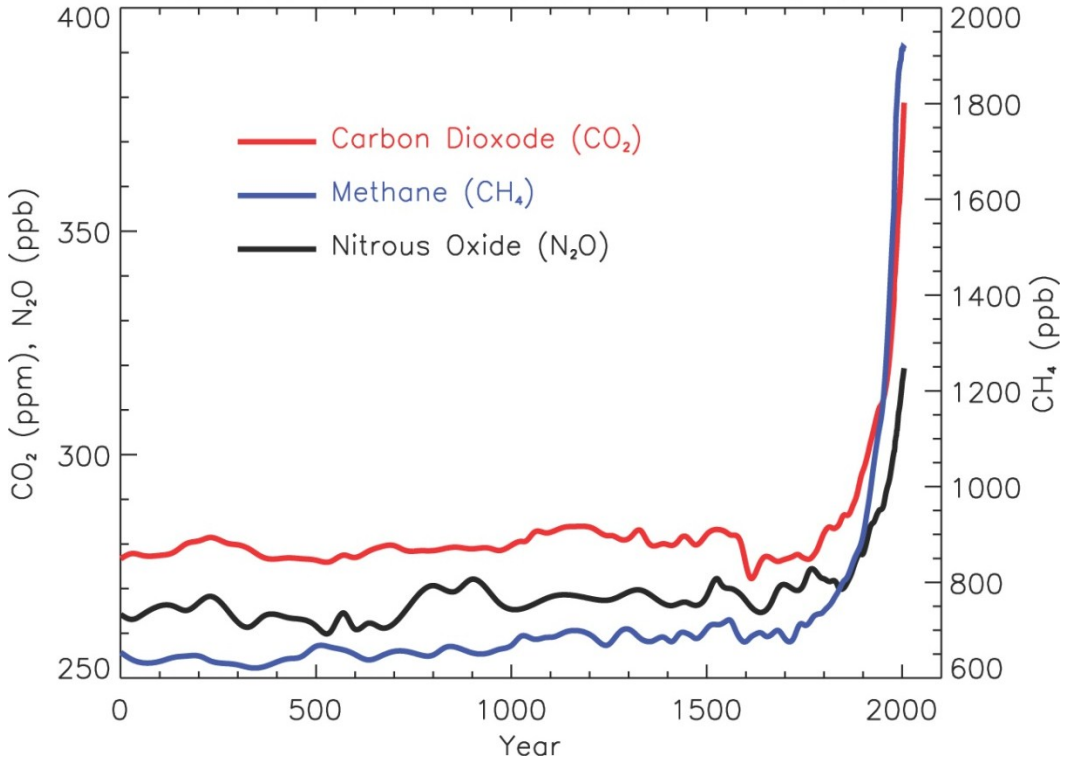


*Figure* 6. Atmospheric Concentrations of Selected GHGs[27]

A global warming gas category is PFCs. These are mostly anthropogenically generated and are particularly potent to climate change. PFCs have been highlighted as some of the more persistent and destructive waste products given off during semiconductor production. The gases listed in Table 2 have been categorized as long-lived greenhouse gases (LLGHG's), and "remain the largest and most important driver of climate change."[27] The atmospheric lifetime of $CO_2$ is 50-200 years while the different compounds generated from the semi-conductor industry have lifetimes of 3,200, 10,000 and 50,000 years for c-$C_4F_8$, $C_2F_6$ and $CF_4$ respectively[27], as shown in Table 2.

To further understand these gases and to compare all substances on an equal basis, a weighted value was established in terms of $CO_2$. The Global Warming Potentials (GWPs) of PFCs are calculated in terms of $CO_2$ equivalent, where its GWP is normalized to 1. The values listed in Table 2 are a sample from the Fourth Assessment Report (AR4)[27], published by the IPCC. The index used is a cumulative radiative forcing between the present and some future time, in this case 100 years. The global warming potentials of PFC's are 5,000 to up to 10,000 times greater than that of $CO_2$. Most of these man-made substances have lifetimes of thousands of years and in the case of $CF_4$, 50,000 years. For this reason, $CF_4$ is a necessary gas to study in regards to its abatement in the semiconductor industry.

Table 2. Global Warming Potentials of PFC, HFC and Other Global Warming Gases, from AR4 [27]

| Greenhouse Gas | GWP for Given Time Horizon | | | Atmospheric Lifetime (yrs) |
|---|---|---|---|---|
| | 20-yr | 100-yr | 500-yr | |
| $CO_2$ | 1 | 1 | 1 | 5 - 200 |
| $CF_4$ | 5,210 | 7,390 | 11,200 | 50,000 |
| $C_3F_8$ | 6,310 | 8,830 | 12,500 | 2,600 |
| $NF_3$ | 12,300 | 17,200 | 20,700 | 740 |
| *c*-$C_4F_8$ | 7,310 | 10,300 | 14,700 | 3,200 |
| $C_2F_6$ | 8,630 | 12,200 | 18,200 | 10,000 |
| $CHF_3$ | 12,000 | 14,800 | 12,200 | 260 |
| $SF_6$ | 16,300 | 22,800 | 32,600 | 3,200 |
| $N_2O$ | 114 | 289 | 298 | 153 |
| $CH_4$ | 12 | 72 | 25 | 7.6 |

PFC gases are used in two primary ways in the semiconductor process. The first use is for the chamber clean process, and the second is for the dielectric etching process.[16] The chamber clean process involves the removal of deposited materials from the walls of chemical vapor deposition (CVD) process chambers. Process etching involves the removal of deposited material from the wafer surface to create a desired circuit pattern.[28] There have been large reductions of PFCs in the chamber clean processes through alternative chemistries and improved methods.[29] Reductions for the dielectric etching process involve abatement in a minor way. Typically, only 20 to 40% of the input gases are consumed in the via-etch processes. The excess gases are subjected to an attempted thermal incineration prior to atmospheric release, where monitoring has demonstrated their increasing presence.[30] These processes have succeeded in the removal of some of the PFC's. However, these steps are inadequate to meet the future EPA 10% reduction goal of 4.41 Tg $CO_2$ Eq. by 2010.[8]

Destruction (abatement) of these exhaust gases is the focus of this study. There are several methods that have been developed to abate the PFC gases. These include, but are not limited to Catalytic – Scrubber and Plasma Units, Thermal Scrubber Units, Atmospheric Plasma Units and Fore-line Plasma Units.[24, 29, 31]

Catalytic abatement units have progressed technologically over the last 15 years. The process uses a solid catalyst material that reacts with the process exhaust gas and the PFC is consumed in the reaction[32]. Several advantages of this process include no formation of incomplete combustion products and no formation of thermal $NO_x$. Brown and Rossin noted in their 2001 article that an obstacle for catalytic abatement was the

catalyst being poisoned by $SiF_4$[32], where the catalyst activity was reduced. Newer technologies combine plasma decomposition with a catalytic immobilization. Suzuki and co-workers (2008) have developed a dual catalytic reaction using $Ca(OH)_2$ /CaO that pre-treats the product gases to immobilize reactive compounds such as $F_2$, $SiF_4$ and $COF_2$[24]. An inductively coupled plasma (ICP) was used to excite the stable compounds $CF_4$, $C_2F_6$ and $C_3F_8$ and immobilized them in the second catalyst column. This process was able to produce a DRE of 99.6% for a flow rate of 200 $cm^3$/min.

Thermal Scrubber units use either combustible gases or an electrically heated chamber to destroy PFC gases[29]. Units are installed after the vacuum pump which has the benefit of not affecting the semiconductor process. In a study of the Edwards TPU4214 system[33], DRE was calculated to be greater than 90%. Unfortunately, this process produced large amounts of $NO_x$ emissions which are highly toxic and strictly monitored. The annual cost of ownership was estimated to be $26,000 per unit[33], which made it cost prohibitive as a viable abatement method.

Plasma Abatement units have many different variations. A partial list includes atmospheric or low pressure, inductively coupled or direct coupled, plasma torches, and microwave generated plasmas or radiofrequency plasmas. Plasma abatement technologies initiate electron dissociation to convert these PFCs into reactive intermediates such as $CF_3$ and $CF_2$.[4] Arno, Bevan and Moisan did early work abating acetone and trichloroethylene using rf plasmas and achieved DREs of 99% for flow rates less than 60 ml/min, but the DRE dropped a flow rates higher than 200 ml/min.[34, 35] Experiments by Xie and colleagues used an atmospheric microwave plasma system to

abate $CF_4$ with a DRE of 98.4%[31]. The Litmas "Blue" system developed by Air Liquide[21] utilized an inductive coupled radio frequency atmospheric abatement system that reported a $CF_4$ abatement DRE of 99%. A foreline PAS was co-developed by Rf Technologies and Texas A&M University that reported a $CF_4$ abatement DRE of 99.9%.[1, 4, 36]

To ensure that the PFCs would not reform, additive gases were inserted into the process stream to force the recombination of the gases into hydrogen fluoride (HF), carbon monoxide (CO), and carbon dioxide ($CO_2$). Hydrogen and oxygen gases were used for the development stages. This was shown by Wofford [4] as

$$60\ CHF_3 + 6\ CF_4 + 70\ Ar + 30\ O_2 + 50\ H_2 \Rightarrow\ HF + CO + CO_2 + H_2O. \qquad \text{Eq (1)}$$

$H_2O$ gas processes were also developed for their low cost and ease of handling[21, 37]. An example is shown by Frantzen[1] as

$$16\ c\text{-}C_4F_8 + 90\ CO + 12\ O_2 + 700\ Ar + xH_2O + 40\ N_2 \Rightarrow HF + CO_2 + CO. \qquad \text{Eq (2)}$$

The first hypothesis of this thesis is that eliminating the forced air convection of the cooling system can maintain system integrity and to reduce the cost of ownership by 50% per year. This is significant because the EPA's semiconductor process fabrication facility rules are estimated to be cost each facility $20 million per year for operating and maintenance.[38] The intent is to reduce the amount of the air used or use a different medium that would produce the same amount of heat transfer. A $C_4F_8$ abatement experiment will run on the liquid cooling design to verify the DRE performance. The second hypothesis is that a semiconductor radio frequency etching reaction of $C_4F_8$ can be simulated using a microwave power source and the products from that reaction can be

abated to greater than 99% DRE. The outcomes of this investigation include a simulation of the radio frequency etching reaction and the abatement of those exhaust gases. The third hypothesis is that a semiconductor radio frequency etching reaction of $CF_4$ can be simulated using a microwave power source and the products from that reaction can be abated using $H_2O$ vapor as the additive gas to greater than 99% DRE. Combining these results with the low cost of ownership, the feasibility of impacting global warming pollution by the semiconductor industry will make this system viable for commercial use.

# 2. DESIGN INVESTIGATIONS OF A PLASMA ABATEMENT SYSTEM

## 2.1. Introduction

A commercial plasma abatement system for use in semiconductor waste treatment gases was developed by Rf Environmental Systems and Texas A&M University. Creating a unit that performs as required is necessary, namely to destroy PFC waste gases from various semiconductor processes. It is secondarily important to reduce the capital cost and/or the reoccurring operational costs. The hypothesis of this experiment is that eliminating the forced air convection of the cooling system can maintain system integrity and to reduce the cost of ownership by 50% per year.

There are two main categories of plasmas, low frequency and high frequency. Low frequency plasmas include: Arcs, Dielectric Barriers, Coronas and Gliding Discharges. High frequency plasmas include: Inductively Coupled Plasmas (ICP), Resonant Cavities and Surface Wave Plasmas (SWP). This current study will focus on SWPs because of certain advantages which include large plasma volumes (plasma length > plasma diameter), broadband impedance matching, a wide domain of operating frequencies, and great stability and reproducibility [39, 40]. The factors that affect gas abatement efficiency are: a) concentration of the gases to be abated, b) electron density and electron energy c) residence time, d) radial contraction of the discharge, and e) gas temperature and reformation rates.[41]

Plasmas can be created by producing a high-frequency discharge using either a radio frequency or microwave power source. A SWP is a type of traveling wave discharge that can be produced within a cylindrical, dielectric discharge tube by an

electrodeless wave launcher. The electromagnetic wave propagates between the surface of this dielectric and the transmitted gas sustaining plasma [42, 43]. When a plasma is created the molecules in the gas can decompose into molecular ions, radicals, individual atoms or even electrons and photons[1, 44]. The reformation of these particles, when they collide in the plasma, is the key to the abatement process which will be further discussed later in the section. A table of different plasma sources and their uses in the semiconductor process are shown in Table 3 below.

Obtaining a surface wave plasma discharge is accomplished when part of the plasma vessel goes into the launching structure. Discharge tubes made of quartz, ceramic or glass, provide the dielectric envelope for the plasma and help to minimize the energy loss[1]. This discharge couples with a dielectric material that encompasses a resonant cavity. There are several variations on the method of coupling the discharge to the resonant cavity. These variations include a surfatron, waveguide-surfatron, and surfaceguide. The differences between the three being that the frequency ranges for the waveguide-surfatron and the surfaceguide have a higher frequency range, $10^9$-$10^{10}$ Hz and the surfatron has a frequency range of $10^8$-$10^9$ Hz. The waveguide-surfatron is an integrated design and the surfaceguide design is a modular design. The latter design was selected to have the widest range of flexibility[39].

Table 3. Plasma Sources and Parameters [45]

| Physics | Pressure (mbar) | $n_e$ ($cm^{-3}$) | $T_e$ (eV) | Bias | Application |
|---|---|---|---|---|---|
| DC glow | $10^{-3}$–100 | | | | |
| Cathode Region | | | 100 | Yes | Sputtering, Deposition, Surface Elementary |
| Negative Glow | | $10^{12}$ | 0.1 | No | Chemistry, Radiation |
| Positive Column | | $10^{11}$ | 1–10 | No | Radiation |
| Hollow Cathode | $10^{-2}$–800 | $10^{12}$ | 0.1 | No | Radiation, Chemistry |
| Magnetron | $10^{-3}$ | | | Yes | Sputtering |
| Arc, Hot Cathode | | | | | |
| External Heating Low Voltage | 1 | $10^{11}$ | 0.1 | No | Radiation |
| Internal Heating | 1000 | $10^{13}$ | 0.1 | No | Radiation Welding |
| Focus | 10 | | keV | | Radiation |
| Rf Capacitive | | | | | |
| Low Pressure | $10^{-3}$–10−1 | $10^{11}$ | 1–10 | Yes | Processing, Sputtering |
| Moderate Pressure | $10^{-1}$–10 | $10^{11}$ | 1–10 | No | Processing, Deposition |
| Hollow Cathode | 1 | $10^{12}$ | 0.1 | No | Processing, Radiation |
| Magnetron | $10^{-3}$ | | | Yes | Sputtering |
| Rf Inductive | $10^{-3}$–10 | $10^{12}$ | 1 | No | Processing, Etching |
| Helicon | $10^{-4}$–$10^{-2}$ | $10^{13}$ | 1 | No | Processing |
| MW | | | | | |
| Closed Structure | 1000 | $10^{12}$ | 3 | No | Chemistry |
| SLAN | 1000 | $10^{11}$ | 5 | No | Processing |
| Open Structure | | | | | |
| Surfatron | 1000 | $10^{12}$ | 5 | No | Processing |
| Planar | 100 | $10^{11}$ | 2 | No | Processing |
| ECR | $10^{-3}$ | $10^{12}$ | 5 | No | Processing |
| Electron Beam | | | | | |
| BPD | $10^{-2}$–1 | $10^{12}$ | 1 | No | Processing |
| Dielectric Barrier Discharge | 1000 | $10^{14}$ | 5 | No | Ozone, Processing Chemistry |

All of these types have the same mode of propagation along the cylinder by the factor, $e^{\mathrm{jm}\varphi}$ where $\mathrm{j}=\sqrt{-1}$, m is an integer and φ is the azimuthal angle[39]. The lowest order is m=0 where the field is independent of φ. The mode m=0 are types of systems further described here.

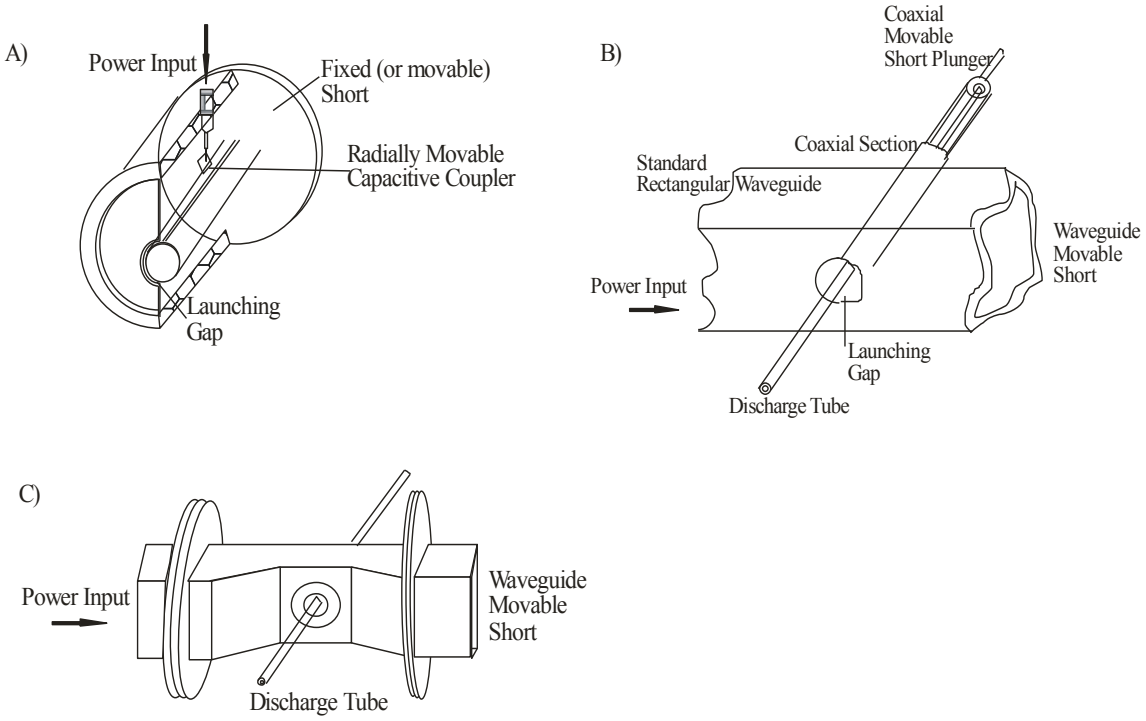


*Figure* 7. Various Types of m = 0 Surface-wave Launchers: A) Surfatron, B) Surfaguide Field Applicator, C) Waveguide-surfatron [42]

The surfaceguide design and theory was developed by Moisan et al. in the early 1980's[40, 46]. He described that the surfaceguide involved a gas that is traveling through the resonant cavity where it is coupled correctly with the high frequency discharge which then ignited into plasma. Three different surface wave launchers are shown above in *Figure* 7. The theory, which is taken directly from his work[46], behind a surfaceguide for a cylindrical dielectric rod aligned parallel to the electric field whose electron density is $N$, critical electron density is $N_c$ has an impedance of $Z_P$. The impedance is characterized by,

$$z_p = Z_p / Z_0 \approx K / (ns + jn) \qquad \text{Eq.(3)}$$

with

$$n = N/N_C, \quad s = \upsilon_{eff}/\omega, \quad N_C = \frac{m\varepsilon_0\omega^2}{e^2} \qquad \text{Eq.(4)}$$

where $j$ is the imaginary operator, $v_{eff}$ is the effective electronic neutral collision frequency for momentum transfer, $m$ and $e$ are the electron mass and charge respectively, and the $\varepsilon_0$ is the permittivity of free space. The shape coefficient K is,

$$K = \frac{a\lambda^2}{\pi^2 d^2 \lambda_g} \qquad \text{Eq.(5)}$$

which depends on the diameter of the plasma column $d$, the free space wavelength $\lambda$, and the waveguide wavelength $\lambda_g$. The dielectric tube impedance is accounted for by $z_D$ for a negligible dielectric loss where the wall thickness of the plasma tube $\delta$, is

$$z_D = Z_D / Z_0 \approx -ja^2 \left[4\pi^2 \delta d (\varepsilon_g - 1)\right]^{-1} \qquad \text{Eq.(6)}$$

The resulting plasma is at a high energy state. When adding other compounds to the process flow, the amount of energy produced is enough to break the molecular bonds of the PFCs. The most stable PFC molecule is $CF_4$ which has a bond strength of 130 kcal/mol[47]. In addition, the breaking of those bonds is accompanied by additive gases to ensure that reformation of the PFCs does not occur. As a result, lower GWP and low molecular weight by-product such as CO, $CO_2$, HF and $H_2O$ are created.

The length of the dielectric tube is dependent on the length of the plasma column, *l*. This is illustrated by *Figure* 8 modified from Moisan and Zakrzewski's review paper[39], where the plasma column travels from $z = 0$ along the z axis. The power flux

*P(z)* decreases and is gradually expended as *z* increases and stops when the wave power drops below the necessary power to sustain the plasma. The amount of power entering the plasma along *z* + *dz* is expressed by defining the wave attenuation coefficient

$$\alpha(z) \equiv -\frac{1}{2}\frac{1}{P(z)}\frac{dP(z)}{dz}. \qquad \text{Eq.(7)}$$

The power per unit length *A(z)* over the distance *z, z* + *dz* is then expressed as

$$A(z) \equiv -\frac{dP(z)}{dz} = 2\alpha(z)P(z). \qquad \text{Eq.(8)}$$

The power loss can be expressed as Joule heating, and under steady-state conditions it is shown as

$$2\alpha(n)P(z)\Delta z = 2\pi \int_0^a \sigma(n)E^2(r)r\,dr\,\Delta z, \qquad \text{Eq.(9)}$$

where *n* is the electron density, *a* is the inner radius of the tube, $\sigma(n)$ is the electric conductivity and *E(r)* is the average total electric field strength of the wave expressed as a function of radius *r*.

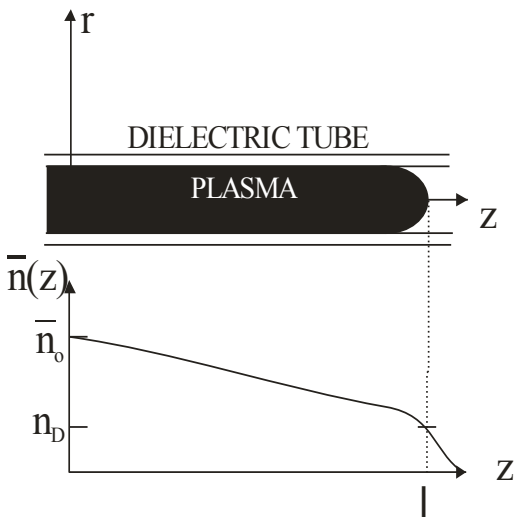


*Figure* 8. Illustration of the Plasma Column and the Cross-Section of Electron Density as the Plasma Travels in the z Direction and Ceases when $z = \ell$

Practically all of the power from the power source is absorbed by the plasma, the power lost per unit length is

$$L(\bar{n})\Delta z \equiv \pi a^2 \bar{n}\theta \Delta z\,, \qquad \text{Eq.(10)}$$

where θ is the power lost per electron. Under steady-state conditions that we are interested in, this leads to $A(\bar{n}) = L(\bar{n})$, which lets us combine Eq.(8) and Eq.(10) to yield

$$2\alpha(\bar{n})P(z) = \pi a^2 \bar{n}\theta\,. \qquad \text{Eq.(11)}$$

Thus we can see how the power source is related to the plasma field, inner diameter of the tube and length of the plasma column.

### 2.2. Experimental

The design parameters for this study focused on cooling the dielectric tube for a commercial application. Existing equipment and parameters were maintained while

performing experiments. The system shown in *Figure 9* consists of a Sairem GMP 20 KSM 2 kW microwave power supply at 2.54 GHz, microwave generator, a circulator, a three stub tuner, and a size WR-430 surfaguide surface wave launcher with a sliding short circuit. The dielectric was a 7.62 cm diameter, 76.2 cm long tube made out of alumina. An Edwards CDP80 dry vacuum pump was used to replicate industrial conditions of the process flow.

The process gases ($CF_4$, $C_4F_8$, CO, $O_2$ and Ar) were added to the system using MKS 1179 mass flow controllers with varying flow rates from 200-1,000 sccm. Water vapor was added to the system via a sealed water vessel using a MKS 1640 mass flow controller. Chilled water was used to cool the microwave generator, circulator and the surfaguide using a 2500 W Neslab CFT-75 chiller. The exhaust gases were passed through a 1.5 gal/min water scrubber to neutralize any HF and $COF_2$ before being vented. Quantitative FTIR measurements using a Bio-Rad FTS 6000 spectrometer equipped with a potassium bromide (KBr) beam splitter and liquid nitrogen cooled mercury tellurite infrared detector was performed on the gases before and after plasma application. One hundred scans were co-added for each spectral scan so that a final spectrum could be generated over the frequency range 700 – 4500 $cm^{-1}$ at 1 $cm^{-1}$ resolution. Other scan parameters included sensitivity setting of 2, a scan speed of 20 kHz, and an aperture setting of 0.25 $in^{-1}$ at 2000 $cm^{-1}$. All gases were passed through a variable path length (2-10 meters) White cell which consists of three gold plated mirrors. The path length was set to 2 meters and the cell was heated to approximately 88 °C. All transfer lines were heated to this temperature to minimize condensation and avoid

adsorption of analytes. The spectra were collected using Bio-Rad Win-IR Pro version 2.0 software with rapid-scan collection, which was used when the product gases were equilibrated.

Exhaust gases were also sampled using QMS, Quadrupole Mass Spectrometry to monitor IR inactive species to determine the percent mass recovery and calculate a balanced chemical reaction. It also provided an independent determination of the accuracy of the measurement for both reactants and products gases studied by the FTIR. The mass spectrometry was performed using a differentially pumped in-situ Leybold Inficon Transpector 200 AMU Residual Gas Analyzer. Spectra were collected by Leybold's TranspectorWare program version 2.01. This system essentially consists of an ion source, quadrupole mass filter, and Faraday cup/electron multiplier detector. The spectrometer was mounted in-line to the vacuum fore-line, meaning the samples were not diluted with the nitrogen purge gas like it was with the FTIR samples. The Transpector 200 AMU Residual Gas Analyzer was equipped with an IPC28 pressure converter, which is an orifice system that allows the sample to be measured at 1 Torr. Typical pressures in the spectrometer ranged from $10^{-6}$ to $10^{-7}$ Torr.

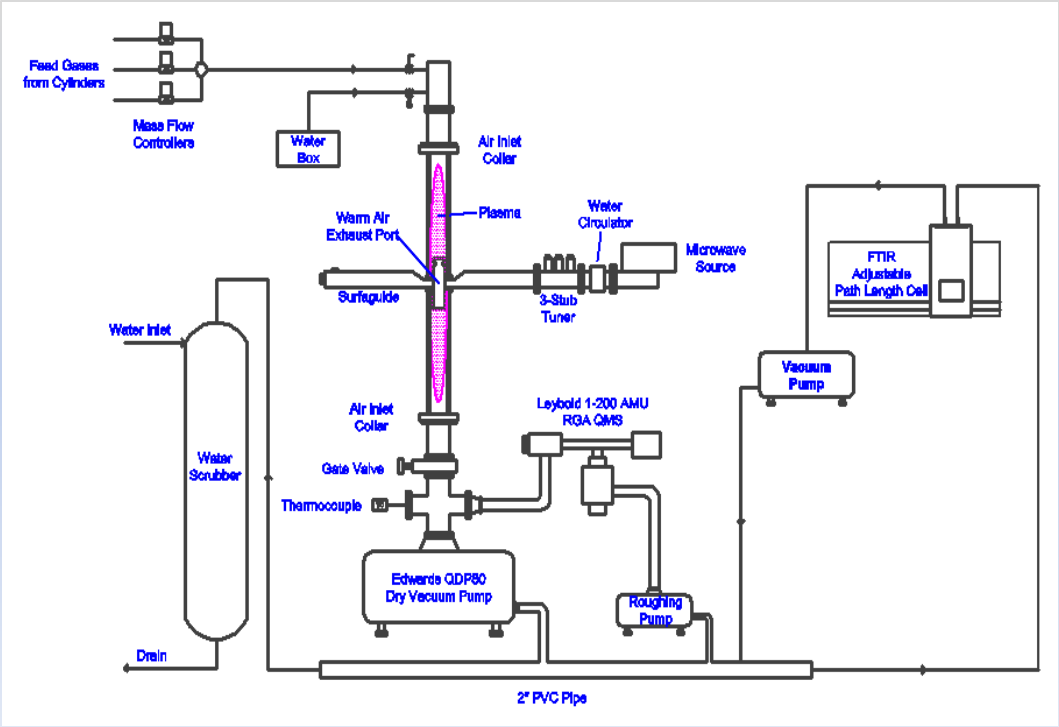


*Figure* 9. Original Plasma Abatement System Schematic

A plasma column was generated inside of the ceramic dielectric tube (*Figure 10*), made of alumina ($Al_2O_3$). When the process gases entered the plasma, the energy from the plasma caused the molecules to dissociate. For example, $COF_2 + e \rightarrow COF + F$, $COF + e \rightarrow CO + F$. This process generated a great deal of heat energy. The physical properties of the ceramic allow for high temperatures and resistance to chemical corrosion. The maximum working temperature for alumina is 1750 °C. It does not absorb water and has no gas permeability.

A vacuum seal around the alumina tube was created using Viton o-rings. They have excellent resistance to fluorinated compounds and a high melting temperature (500 °C). A requirement for the cooling system is that it adequately cools the alumina tube

and the o-rings. An even temperature distribution will produce an even thermal expansion of the ceramic. This will ensure that the ceramic does not develop stress fractures.

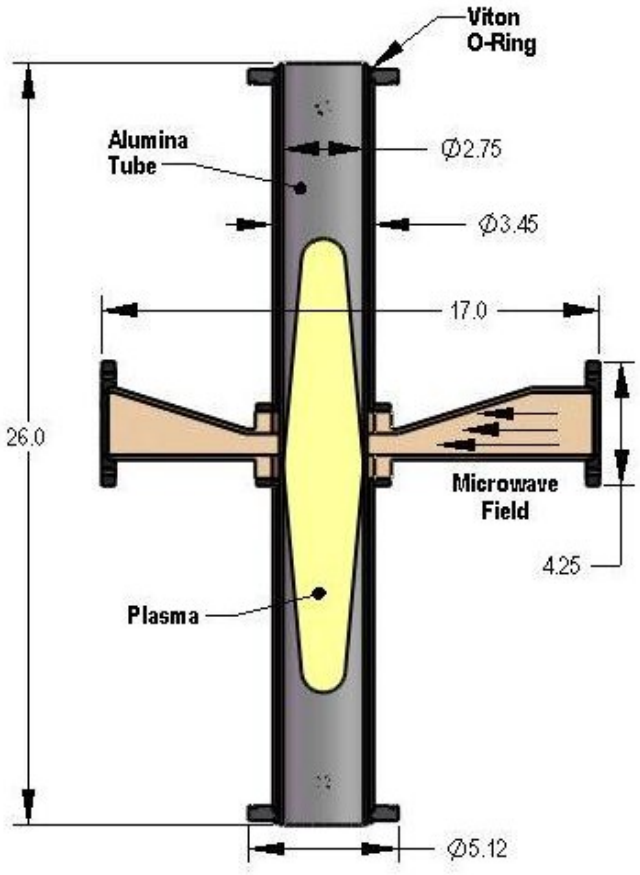


*Figure* 10. Abatement System Ceramic Tube Cross-section

### 2.3. Results and Discussion

The length of the dielectric tube was determined experimentally by Bela Derecskei[48] using the DRE (destruction removal efficiency) of the system for $CF_4$ at 100 sccm and 2kW power. Lengths of tube 45.7, 50.8, 61.0 and 76.2 cm were tested.

Based on the results shown in *Figure 11*, a tube length of 66 cm was selected as the optimal length.

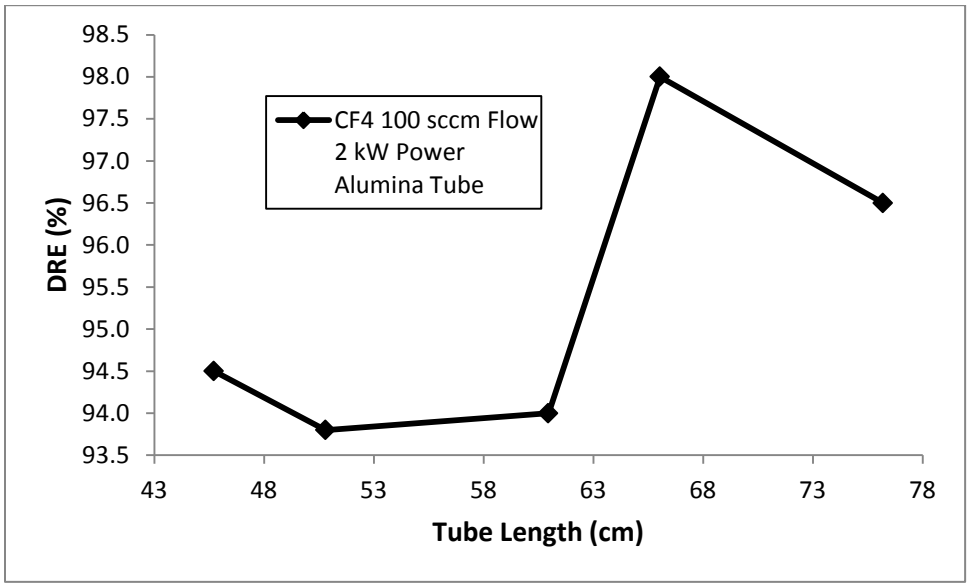


*Figure* 11. Dielectric Tube Length vs. $CF_4$ Destruction Removal Efficiency

The amount of cooling needed for the system is determined by calculating the amount of heat removed from the system. The method of cooling used forced convection between concentric tubes. Input air lines with a total rate of 510-595 lpm were attached at each end of the tube and an output port was constructed in the middle of the tube. Any improvements made must be based on the heat dissipation of this standard design. An energy balance on the tubes provides the amount of cooling:

$$\dot{Q} = (\dot{m}C_p)_c (T_{c,o} - T_{c,i}) . \qquad \text{Eq.(12)}$$

Temperatures were measured using type K thermocouples and the measured input and output temperatures for the air were 22°C and 80°C, respectively. The mass flow rate, $\dot{m}$ was 0.01168 kg/s and the average specific heat for the temperature range was 1009

J/kg°C. This gave a result for the heat flow rate ($\dot{Q}$), to be 683 W. This was approximately the heat energy that must be removed from the system.

To achieve the equivalent amount of cooling with a lower flow rate of cooling air, multiple modes of heat transfer must be evaluated. There are three modes of heat transfer: convection, conduction and radiation. By including radiation, the amount of heat dissipated can be increased with using less air flow.

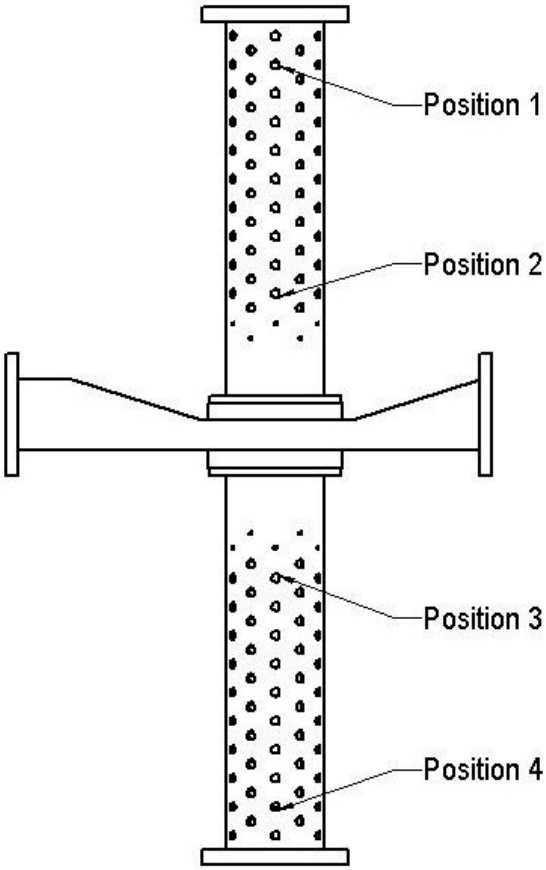


*Figure* 12. Brass Chimneys with Air Vents

Holes were added to the brass chimneys as shown in *Figure 12*. This allowed the heat energy to be emitted from the ceramic tube directly into the ambient room. Special consideration was made for the size and distance of the air vent from the microwave coupling region. As the microwaves pass through the surfaguide and couple with the process gases in the dielectric tube, some of the microwaves propagate along the tube. The vent hole must be smaller than ∅0.8 cm, more than 8 cm from the surfaguide and smaller than ∅0.3 cm less than 8 cm otherwise microwaves are emitted out of the system.

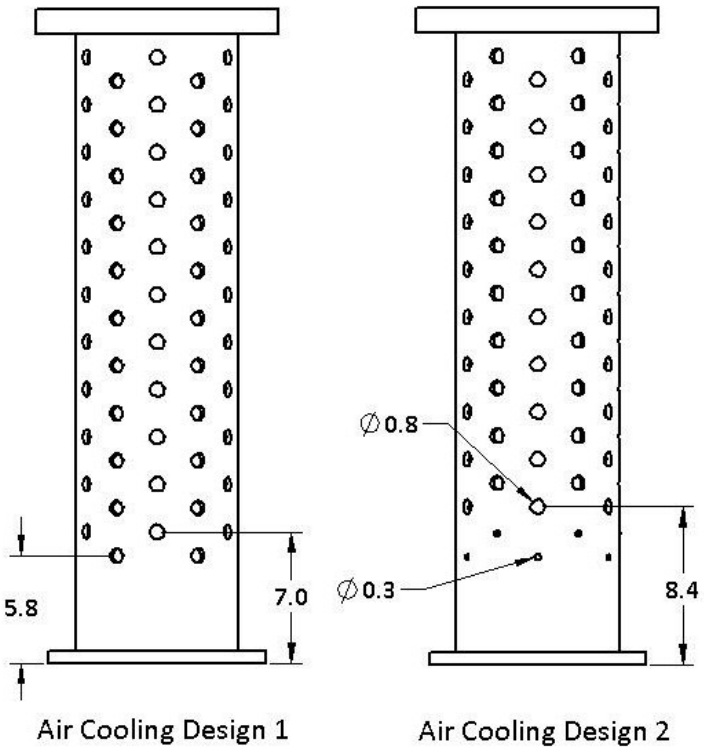


*Figure* 13. Chimney Air Cooling Designs

The microwave power supply operates with a frequency of 2.54 GHz and the following equation can be used,

$$\lambda = c/\nu, \qquad \text{Eq.(13)}$$

where λ is the wavelength, c is the speed of light and ν is the frequency, which gives a wavelength of 12.23 cm. The electric field generated is not able to propagate through the holes that are much smaller than the 12.23 cm wavelength. The field that does penetrate through larger holes dies off exponentially as the distance from the chimney increases. *Figure 13* shows the two air cooling design chimneys. Measuring the microwave leakage on design 1, the largest measurement with a ∅0.76 cm hole 7 cm below the surfaguide was 2.0 mW/cm$^2$ at a radial distance of 0-5 cm from the chimney. A vertical distance of 7.5 cm from the surfaguide is the critical region. The highest density electric field region had the largest leakage per hole. Therefore, at a distance less than 7 cm above and below the surfaguide the holes were ∅.32 cm. Beyond 8.4 cm a hole of ∅0.76 cm could be used with negligible microwave leakage.

Initial testing of a 1950W microwave plasma using 60 sccm of Argon and 130 sccm of $H_2O$ as shown in *Figure 12*, showed temperatures well below critical temperatures for either the o-rings or the ceramic tube, 500°C and 1750°C respectively. Measurements were recorded over 130 hours at four positions on the ceramic tube. Temperature was measured using a Type K thermocouple probe. Temperatures on the external surface of the tube were below the critical temperature for the ceramic of 1750°C.

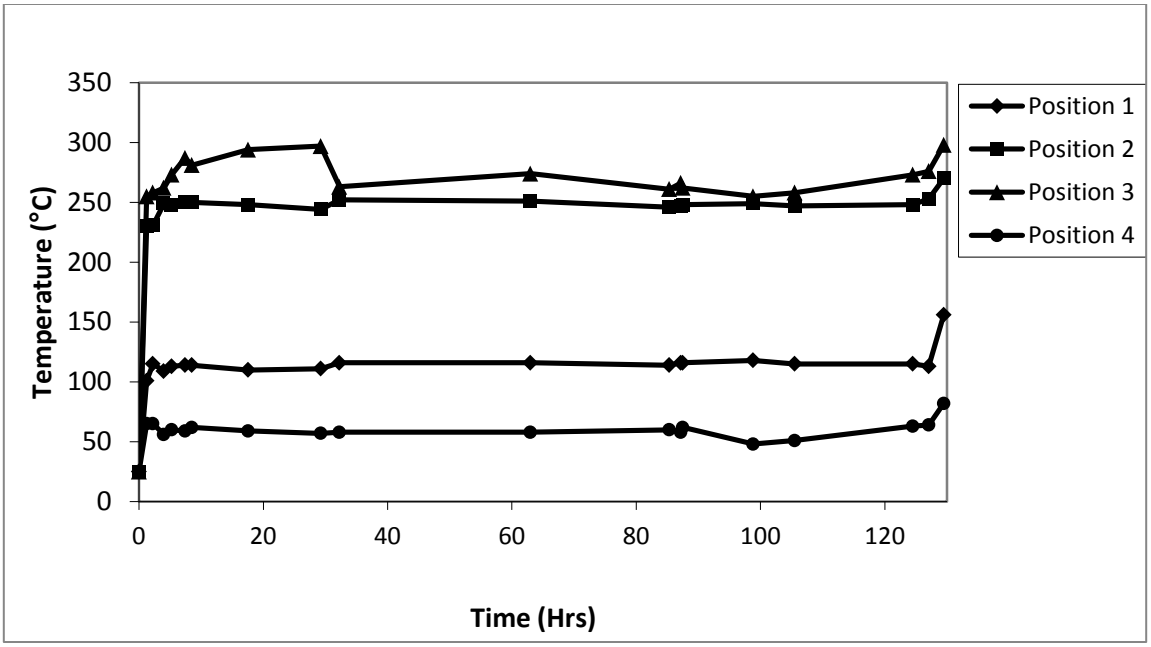


*Figure* 14. Ceramic Tubing Cooling with No Air Cooling

The data in *Figure 14* shows that the hottest temperatures were at Positions 2 and 3. Although this was a good indication of the outer temperature of the ceramic tube, approximately 11.4 cm on either side of the surfaguide were not able to have temperature measurements taken due to the microwave radiation. An approximation must be made to the maximum outer temperature of the tube before a calculation of the inner temperature can be made.

Measuring the surface temperature of the ceramic tube along the tube using six data points, a curve can be plotted above and below the surfaguide. *Figure 15* shows distances above the surfaguide in negative numbers and distances below the surfaguide in positive numbers. Temperatures below were greater than those above, so the maximum approximated temperature was 2.5 cm below the surfaguide. Using a smooth curve fit, the maximum temperature at this location was estimated to be 394°C.

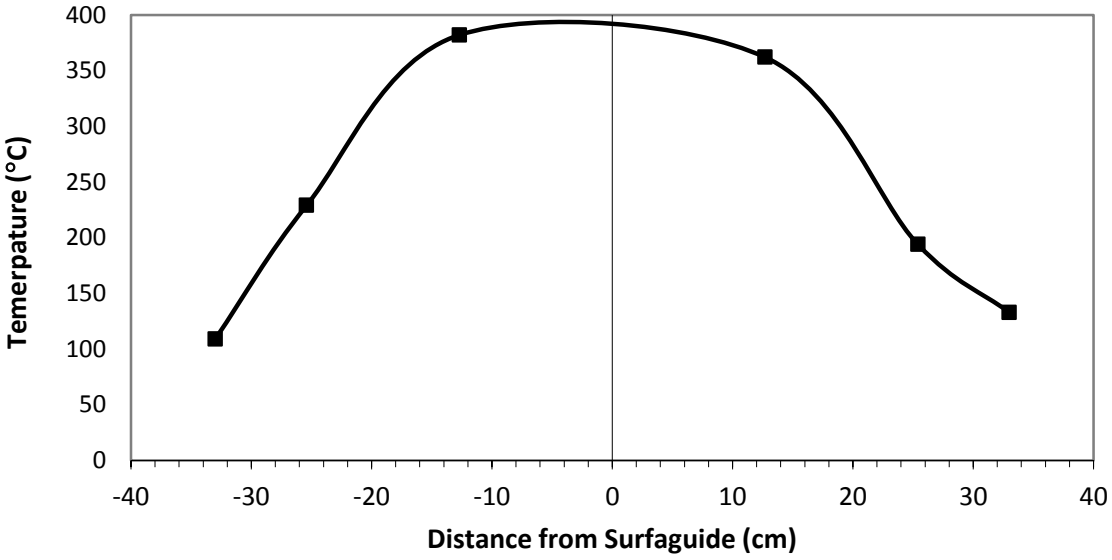


*Figure* 15. Surface Temperature Profile Along Alumina Tube

Once a maximum theoretical temperature was determined, the maximum temperature on the inside of the tube can be calculated. Examining the section of the tube that the microwaves were penetrating, we can use a form of Fourier's law[49], where,

$$\dot{Q} = Aq = 2\pi Lr\left(-k\frac{dT}{dr}\right), \qquad \text{Eq.(14)}$$

and for a cylinder[49],

$$\dot{Q} = \frac{2\pi kL(T_1 - T_2)}{\ln(r_2/r_1)}. \qquad \text{Eq.(15)}$$

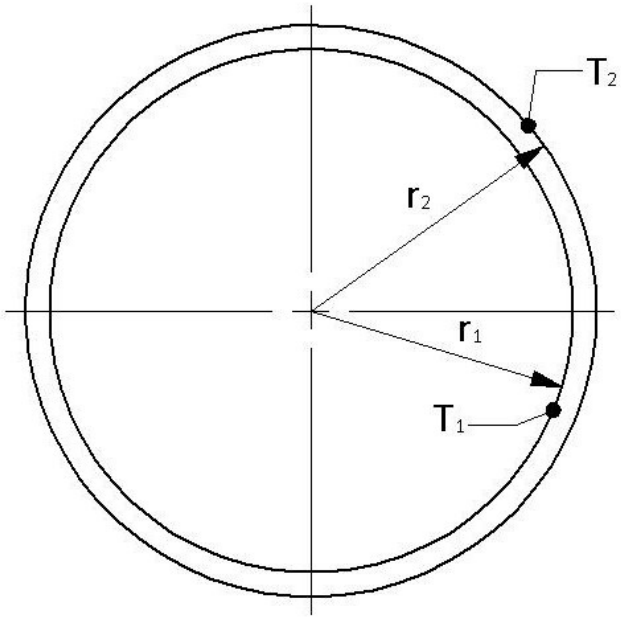


*Figure* 16. Cylinder Cross-Section

The thermal conductivity at 600 K was 16 W/m*K. The length of L was 0.0254m. The radii of $r_1$ and $r_2$ , as shown in *Figure* 16 above, were 0.0698m and 0.0792m, respectively. The heat transfer $\dot{Q}$ was assumed at a maximum of 2000W because that was the maximum power emitted from the microwave. Solving this equation, with a value for $T_2$ of 394°C, resulted in a temperature of $T_1$ of 463°C. This was well below the maximum usable temperature of 1750°C specified by the manufacturer.

Unfortunately, experiments with a zero air flow rate using only ambient cooling lasting more than ten days resulted in tube failure. Catastrophic failure was often the result of weakening of the tube wall through high temperature differentials. The tensile stress due to thermal expansion is defined by

$$\sigma = -E \cdot \alpha \cdot \Delta T \qquad \text{Eq.(16)}$$

where E is the modulus of elasticity, a is the coefficient of thermal expansion and ΔT is the temperature differential. Alumina has a tensile strength of 248 MPa, an E of 370 GPa and a of 8.2 x $10^{-6}$/°C, which then calculated to a maximum temperature differential of 82°C. Maintaining the temperature differential along the tube was determined to be of critical importance. Therefore, reducing the air flow rate caused a temperature difference that led to stress greater than the materials' properties. The cooling of the system using ambient air without forced convection was determined to be unrealistic.

A new cooling design was conceived using liquid cooling. Water would be an ideal choice, but water molecules have a dielectric constant of approximately 80. This causes them to become excited by microwaves. Therefore, chilled water cannot be used for cooling. For the microwaves not to be absorbed by the coolant, it must have a low dielectric constant. Air has a dielectric constant of 1.0059, so to nearly approximate it, a fluid must have a value close to that of air. The dielectric constant of alumina is 9.8 and for the selected fluid (Galden HT 200) it is 1.94. Using a liquid cooling design allowed the system to be contained without having to vent the hot gases. A liquid cooled design allowed for a greater heat transfer coefficient with less volume passing through the system. A cross-section of the design is shown in *Figure* 17 below.

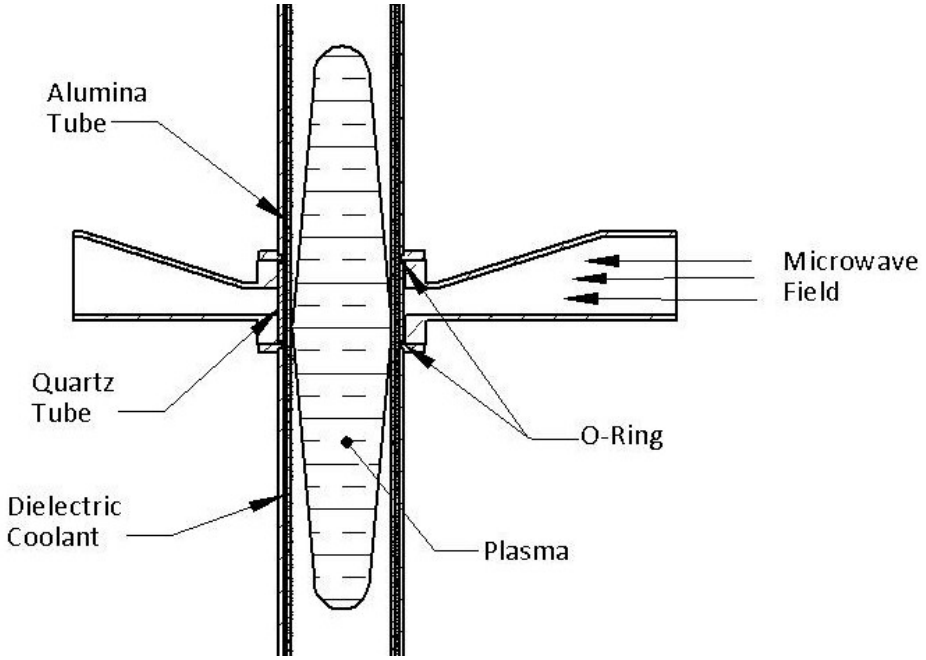


*Figure* 17. Liquid Cooling Design Cross-Section

To determine which fluid would be best, a study of the heat transfer had to be done. The method of heat transfer from the ceramic tube to the cooling fluid was convection. The rate of heat transfer for convection was,

$$\dot{Q} = \bar{h}_c A_s (T_s - T_e) . \qquad \text{Eq.(17)}$$

Similar to Equation Eq.(12) where $\dot{Q}$ was the rate of heat transfer [W], $A_s$ was the surface area, $T_s$ and $T_e$ were the surface and fluid temperatures respectively, and $\bar{h}_c$ was the heat transfer coefficient. The surface area was simply

$$A_s = \pi DL , \qquad \text{Eq.(18)}$$

and had a value of 0.158 $m^2$.

To determine $\bar{h}_c$ the type of flow must be found. Using the equation for Reynolds number of

$$\mathrm{Re}_D = \frac{\dot{m} D_h}{A_c \mu}, \qquad \text{Eq.(19)}$$

the type of flow, laminar or turbulent can be determined. A flow rate of 14.0 l/min would result in a mass flow rate ($\dot{m}$) of 0.113 kg/sec for a density (ρ) of 1790 kg/m$^3$. The hydraulic diameter ($D_h$) was used in irregular shapes and is defined as

$$D_h = \frac{4A_c}{\wp}. \qquad \text{Eq.(20)}$$

The value for $A_c$, the cross-sectional area of flow was 7.913e$^{-4}$ m$^2$. The value for $\wp$, the wetted perimeter was 0.498 m. Thus, $D_h$ was 6.35e$^{-3}$ m. Knowing the kinematic viscosity ($\nu$) from the vendor literature, the dynamic viscosity (μ) of 4.296e$^{-3}$ m$^2$/s was found. Using these equations, the Reynolds number ($Re_{Dh}$) was found to be 780. For $Re_{Dh}$ <2800, the flow was laminar. The low flow rate and the small hydraulic diameter allows calculating the average Nusselt number ($\overline{Nu}_{D_h}$) to approximate flow between isothermal parallel plates[49]:

$$\overline{Nu}_{D_h} = 7.54 + \frac{0.03\left(D_h/L\right)\mathrm{Re}_{D_h}\,\mathrm{Pr}}{1 + 0.016\left[\left(D_h/L\right)\mathrm{Re}_{D_h}\,\mathrm{Pr}\right]^{2/3}}. \qquad \text{Eq.(21)}$$

The Prandlt number ($Pr$) is defined by

$$Pr = \frac{c_p \mu}{k}. \qquad \text{Eq.(22)}$$

The values for specific heat ($c_p$), dynamic viscosity ($\mu$), and thermal conductivity (k) were 963.0 J/kg*K, 4.296e$^{-3}$ m$^2$/s and 0.07W/m*K, respectively. Substituting these values into Equation Eq.(22) yielded 59.1. Solving for Equation Eq.(21), the Nusselt number was 8.23. A Nusselt number correction factor recommended by Petukov and Roizen[49] for annular ducts was

$$0.86\left(\frac{D_i}{D_o}\right)^{-0.16}, \qquad \text{Eq.(23)}$$

where $D_o$ and $D_i$ were the outer and inner diameters respectively. A correction factor of 0.87 multiplied by the old $Nu_D$ yielded a and new $Nu_D$ of 7.15.

Finally the Nusselt number was defined as

$$\overline{Nu}_D = \frac{\bar{h}_c D_h}{k}, \qquad \text{Eq.(24)}$$

for forced and natural flows[49]. Solving for $\bar{h}_c$ gave a result of 78.9 W/m$^2$*K. Assuming again that all of the power was transferred to heat energy, Equation Eq.(17) can be solved for the change in temperature between the surface temperature of the tube, $T_s$ and the cooling fluid temperature, $T_e$ resulting in a $\Delta T$ of 160°C. The surface temperature of the ceramic tube using high air flow cooling was 323°C. This gave a bulk temperature for the dielectric fluid of 163°C, which was below the maximum service temperature of 473°C.

The final design consisted of housing the PAS inside of a 61x91x183 cm steel rack. The plasma waveguide assembly was mounted along with the liquid cooling

system as shown in *Figure 18*. Access ports were given to the input and output lines for the PFC gases. A mass flow controller and a water mass flow controller previously described were installed to regulate the additive gases of Argon and water vapor. A copper brazed-plate heat exchanger with a cooling capacity of 17 kW was used to cool the dielectric fluid. A reservoir with a capacity of 7.6 liters measuring 25 x 25 x 20 cm was installed.

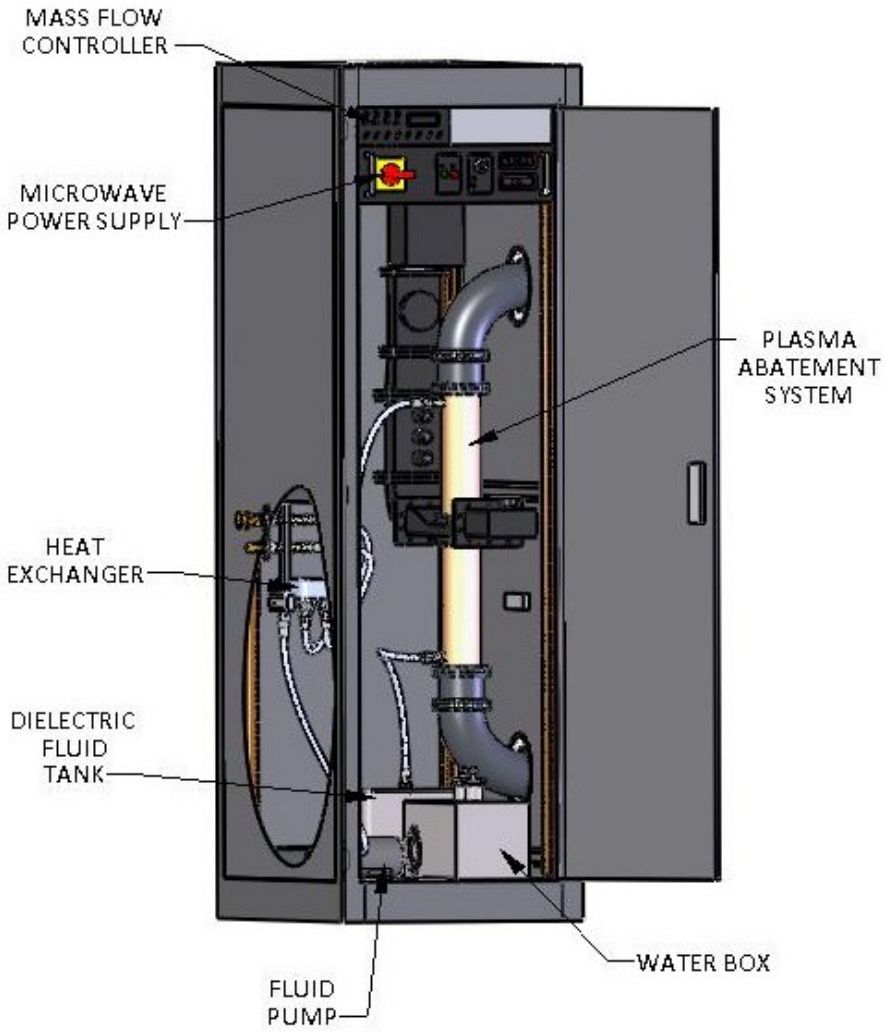


*Figure* 18. Packaged Plasma Abatement Design

The cost of ownership (COO) for the PAS was originally calculated on the laboratory alpha model design. It had a cost of $50,000 with a commercial version estimated at $35,000[36, 50]. Utility and consumable cost projections were made on certain baseline assumptions. The primary utilities would be electricity, industrial chilled water, cooling air, hydrogen and oxygen. The system would operate at 1kW of applied power. In-house dry air could be circulated through the system and exhausted. Chilled house water could be used for the dielectric tube, microwave head, and generator.

A hypothetical etch period of 210 seconds, 210 etch cycles per week, 637 hours per year of operation on a typical chamber was selected. Annual maintenance included replacement of Viton o-rings and the ceramic tube and costs of $32 and $250 respectively. A detailed utility cost comparison is shown in Table 4. Design A shows the figures listed by Vartanian, and Wofford et al [36] during its evaluation at the SEMATECH conference in 1998. The utility rates have been adjusted to reflect current prices where known.[51]

The most significant improvement is in the cooling air exhaust. The need for air as a means of cooling the system significantly reduced the cost of ownership of the system by 90%.

Table 4. Utility Cost Comparison

| Design | Utility | Consuption | Total Amount | | Unit Cost ($) | | Total Cost |
|---|---|---|---|---|---|---|---|
| A | Electrical | 1.5 kW/hr x 637 hr | 955.5 | kW | 0.11443 | /kW | $109.34 |
| | Industrial Chilled Water | 1 gal/min x 60 min/hr x 637 | 38220 | gal | 0.001 | /gal | $38.22 |
| | Hydrogen | 0.0018 cf/min x 60 min/hr x 637 hr | 68.8 | cf | 0.026 | /cf | $1.79 |
| | Oxygen | 0.0011 cf/min x 60 min/hr x 637 hr | 42 | cf | 0.03 | /cf | $1.09 |
| | Cooling Air Exhaust (Clean Dry Air) | 15 cf/min x 60 min/hr x 637 hr | 573,300 | cf | 0.00244 | /cf | $1,398.85 |
| | Air Conditioning Load | 1.43 BTU/min x 60 min x 637 hr | 54,654 | BTU | 0.00001 | /BTU | $0.49 |
| | | | | | Total | | $1,549.78 |
| B | Electrical | 1.5 kW/hr x 637 hr | 955.5 | kW | 0.11443 | /kW | $109.34 |
| | Industrial Chilled Water | 1 gal/min x 60 min/hr x 637 | 76440 | gal | 0.001 | /gal | $76.44 |
| | Water Vapor[1] | 0.08 L/min x 60 min/hr x 637 hr / 3.207 $L_{vapor}$ / $L_{liquid}$ | 0.953 | $L_{liquid}$ | 1.50 | /L | $1.43 |
| | Air Conditioning Load | 1.43 BTU/min x 60 min x 637 hr | 54,654 | BTU | 0.00001 | /BTU | $0.49 |
| | | | | | **Total** | | **$149.48** |

[1] Calculation for 1 ml liquid water equates to 3207 ml of water vapor.

The final PAS design incorporated all of the major design considerations that were specified: A low cost system that was easy to manufacture, inexpensive to maintain, a cooling system that was adequate yet inexpensive to operate and a small foot print for the semiconductor facilities. All of these specifications were met while maintaining the abatement effectiveness of the original laboratory model.

### 2.4. Design Verification

Verification of the design changes was performed by running an abatement reaction though the system. The setup procedures are fully explained in Section III. The dielectric cooling fluid was circulated using a 14.4 lpm capacity impeller pump. The total head of the system was approximately 12 kPa and a flow rate of 14.0 lpm. Chilled

water was circulated through the plate heat exchanger at 25°C. The reactants were as shown,

$$35\ c\text{-}C_4F_8 + 15\ O_2 + 500\ Ar + 90\ H_2O\,. \qquad \text{Eq.(25)}$$

The temperature of the dielectric tube was maintained below 100 °C by measuring the cooling fluid's temperature. The power on the microwave source held constant at 1935 W and the amount of water vapor was altered to determine the optimal DRE value as shown in Table 5. The completed results of the experiment are shown in Table 6. The test results show that the maximum service temperature of the dielectric coolant was 43°C. This was much less than the calculated maximum value of 160°C. Thus the goal of cooling the system was successful using a liquid cooling design.

Table 5. Liquid Cooling Abatement Experiment Matrix

| Run | Microwave Power[a] (W) | $H_2O$ Added[b] (sccm) |
|---|---|---|
| 1 | 0 | 70 |
| 2 | 1,935 | 70 |
| 3 | 1,935 | 80 |
| 4 | 1,935 | 90 |
| 5 | 1,935 | 100 |
| 6 | 1,935 | 110 |
| 7 | 1,935 | 120 |
| 8 | 1,935 | 130 |
| 9 | 1,935 | 140 |
| 10 | 1,935 | 150 |
| 11 | 1,935 | 160 |

a - Power stability ± 0.1%
b - Flow rate error ± 1% of full scale

Table 6. Temperature Verification Results

| Measurement | Time[a] (min) | Microwave Power[b] (W) | Coolant Temp[c] (°C) |
|---|---|---|---|
| 1 | 0 | 0 | 25.2 ± .1 |
| 2 | 12 | 1,935 | 36.2 ± .1 |
| 3 | 22 | 1,935 | 40.0 ± .1 |
| 4 | 33 | 1,935 | 42.6 ± .1 |
| 5 | 40 | 1,935 | 43.3 ± .1 |
| 6 | 50 | 1,935 | 43.3 ± .1 |
| 7 | 60 | 1,935 | 41.8 ± .1 |
| 8 | 68 | 1,935 | 41.3 ± .1 |
| 9 | 80 | 1,935 | 40.8 ± .1 |

a - Time measurements ± 0.5 minutes
b - Power stability ± 0.1%
c - Temperature measurements ± 0.1 °C

The FTIR data was collected for this experiment using the equipment previously described. The absorbance spectra for each run were recorded. Three spectra were recorded for each run. Integration, using BOMEM Grams/32 software, was performed for the absorbance area under the curve for the range of 1369-1310 $cm^{-1}$, to analyze $C_4F_8$. The average of the three runs was then applied against a known calibration gas.

A calibration matrix for each product and by-product gas was generated by measuring the absorbance of selected ro-vibrational features of differing concentrations of each gas diluted in nitrogen. Concentrations of each certified calibration standard gas were selected with a concentration of 1-10% to accurately cover the range of measured concentrations of abated products. Calibration curves were then generated to covert measured absorbance from the FTIR to parts per million (ppm) of a specific gas. This data was fit to a known calibration curve for $C_4F_8$ diluted 1% in $N_2$. The calibration curve was created by integrating the same area for known mass flow rates and a best fit

curve was applied, see APPENDIX B. The experimental data was then applied to the best fit curve.

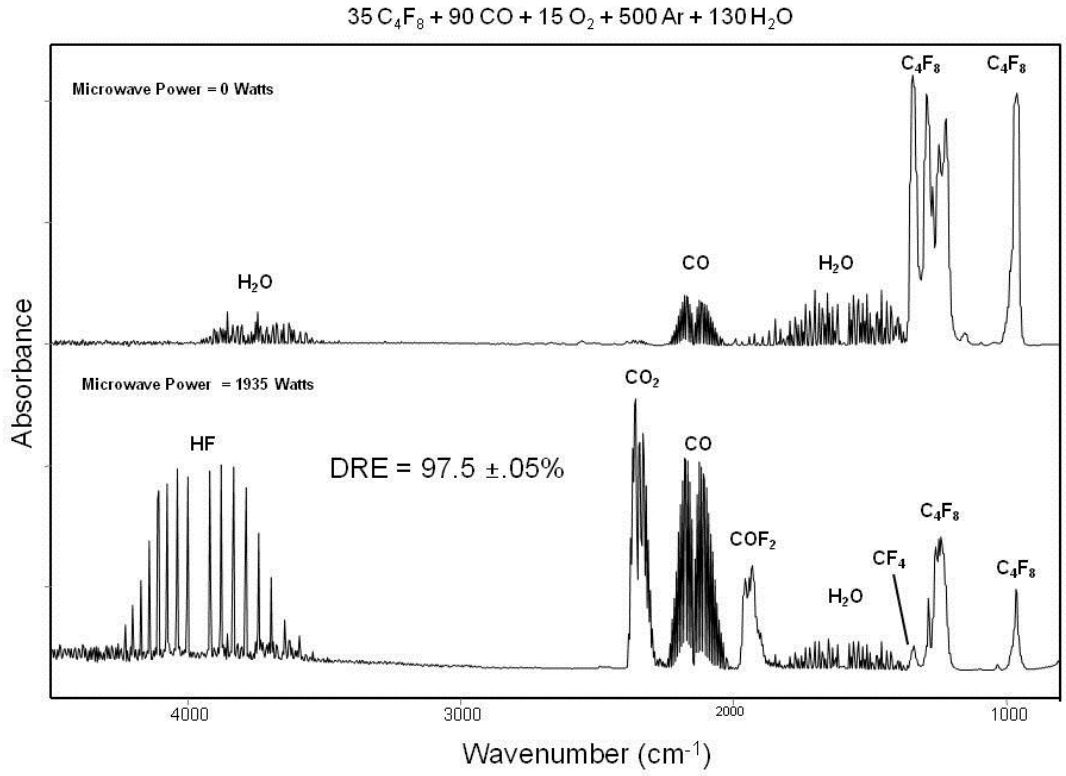


*Figure* 19. Liquid Cooling Design Spectra

*Figure 19* shows the spectrometer results from this experiment. The top line represents the process gases only. The bottom line shows the highest achieved DRE of 97.6 ±.05% for $C_4F_8$ at 130 sccm of $H_2O$ vapor. It did however create $CF_4$ in the process, which was not completely abated. The value was ~2% lower than previous experiments. The efficiency was probably affected by adding another dielectric material in the microwave field, resulting in a less efficient microwave coupling interaction. This system overall was thermally stable and self contained.

# 3. A DETAILED STUDY OF THE ABATEMENT OF POST SILICON OXIDE ETCHING USING OCTOFLUOROCYCLOBUTANE ($C_4F_8$) GAS

## 3.1. Introduction

Experiments were performed to determine the abatement effectiveness of destroying octofluorocyclobutane ($C_4F_8$) as a pure gas, but not when etching silicon[1]. The purpose of this study was to simulate radio frequency (≈1-300 MHz) etching plasma using microwave frequency (300MHz – 10 GHz) etching plasma and then abate the waste gases produced ($SiF_4$, CO, $CO_2$, $COF_2$, $CF_4$) by using another microwave frequency (300MHz – 10 GHz) etching plasma. The resulting DRE should correspond to previously publish data. The hypothesis of this section is that a semiconductor radio frequency etching reaction of $C_4F_8$ can be simulated using a microwave power source and the products from that reaction can be abated to greater than 99% DRE.

$C_4F_8$'s purpose in the CVD etching process was to react with the silicon wafer and remove selected sections. Estimates of unreacted $C_4F_8$ in the oxide etch process were 25%[30]. In fact, $C_4F_8$ decomposed into other PFCs in which some had a higher GWP and atmospheric lifetime than that of the principle. This makes the study of the reacted PFC necessary.

Experiments were performed to simulate the semiconductor etch process. This generated the products that were necessary for a complete abatement study. Previous studies have examined the abatement effectiveness on the source gases[1]. This study included the addition of silicon in the form of $SiO_2$. The CVD etching (or patterning)

process uses plasma generated fluorine atoms which chemically react with the dielectric film to selectively remove specific portions[8]. The CVD etching process used a radio frequency (RF) plasma at 13 MHz, while the simulation involved the use of a microwave plasma at 2.54 GHz. This difference did not allow for an exact replica of the semiconductor conditions, but it produced the necessary products, namely $SiF_4$, that were needed for a more complete simulation reaction process. The fluorine atoms produced by the etching plasma reacted with the silicon in the quartz dielectric tube to form silicon-tetrafluoride, $SiF_4$. The amount of $SiO_2$ in the reactant equation was unknown because it was taken from the quartz tube wall, but it was indirectly measured as the amount of $SiF_4$ in the products equation. Thus, the simple plasma etch reaction hypothesized to be of the form,

$$c\text{-}C_4F_8 + O_2 + CO + Ar + SiO_2 \rightarrow SiF_4 + CO + CO_2 + COF_2 + CF_4, \quad \text{Eq.(26)}$$

and some of the reactants for the simple abatement reaction was then hypothesized to be of the form,

$$SiF_4 + CO + CO_2 + COF_2 + CF_4 + H_2O_{\text{added}} \rightarrow HF + CO + CO_2 + SiF_4. \quad \text{Eq.(27)}$$

### 3.2. Experimental

The simulated manufacturing recipe was given in standard cubic centimeters per minute (sccm) of each process gas. Water vapor was an additive gas used in the abatement process to produce the more favorable byproduct from the fluorine ion, hydrogen fluoride (HF). This prevented the reformation of another PFC molecule because the dissociation energy of the H-F bond is 552.6 kJ/mol and stronger than the dissociation energy of the C-F bond, 485.6 kJ/mol.

The apparatus setup consisted of two abatement systems in-line with each other. The majority of the system was identical to the apparatus setup shown in *Figure 9*, with the addition of another microwave and dielectric tube, *Figure 20*.

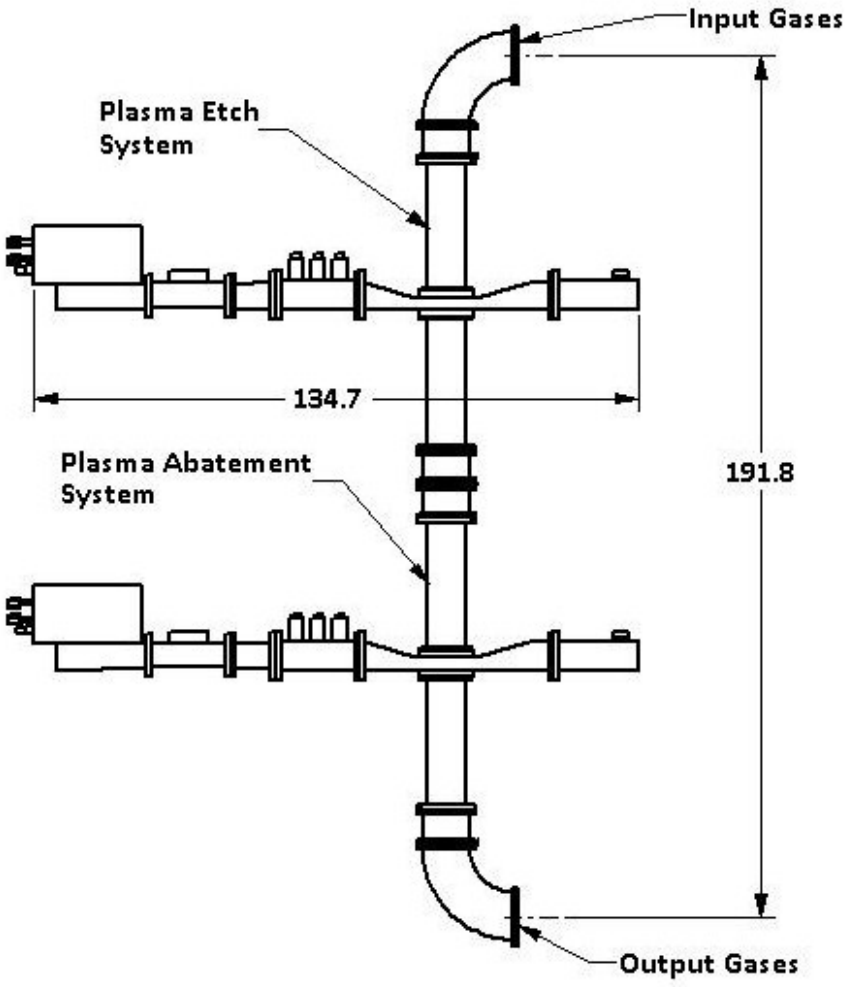


*Figure* 20. Semiconductor Abatement Simulation Setup

The dielectric tube used in the first system, identified as etch system, was quartz. It had an outer diameter of .64 cm and a length of 66 cm. Quartz has the same molecular makeup ($SiO_2$) as silicon wafer thin films used in the semiconductor patterning

process[8]. Creating plasma in this system with a quartz tube caused the fluorine to etch the silicon from the tube. This is shown by the reaction

$$4\ F^- + SiO_2 \rightarrow SiF_4 + O_2. \qquad \text{Eq.(28)}$$

The products from Eq.(26) simulated the products from the semiconductor etch tool. These then were the reactants in the second abatement system, Eq.(27).

To accurately determine the DRE of the system on $C_4F_8$ the waste gases from a semiconductor facility or a close approximation must be used. The semiconductor industry's radio frequency power process has a published consumption ranging from 20-40% for $NF_3$ and $SF_6$ but varies depending on power levels and flow rates[52] each tool, company or process used. Certain reactions involving $CF_4$ and $CHF_3$ actually produced as much as 300% more $CF_4$ during the etching plasma reaction. An etching power experiment was performed with the process recipe at different power levels to ascertain a suitable microwave power approximation. Using the same method describe in the previous section, a calibration curve was applied to this data. *Figure* 21 shows the results of this test. At the 500W power level $C_4F_8$ was dissociated partially to react with the $SiO_2$ to form $SiF_4$ with a DRE of 78.5%. Multiple PFC gases were produced; among them are $C_2F_4$, $CF_4$, $C_2F_6$ and $COF_2$. At the 1000W power level $C_4F_8$ increased its' DRE to 95.4% with the continued formation of PFC gases. The 1500W and 2000W power levels showed a dramatic drop off of most species excluding $SiF_4$. For this determination of a RF plasma, the last two power settings were excluded. The 1000W setting was selected because it produced lower concentrations of PFCs.

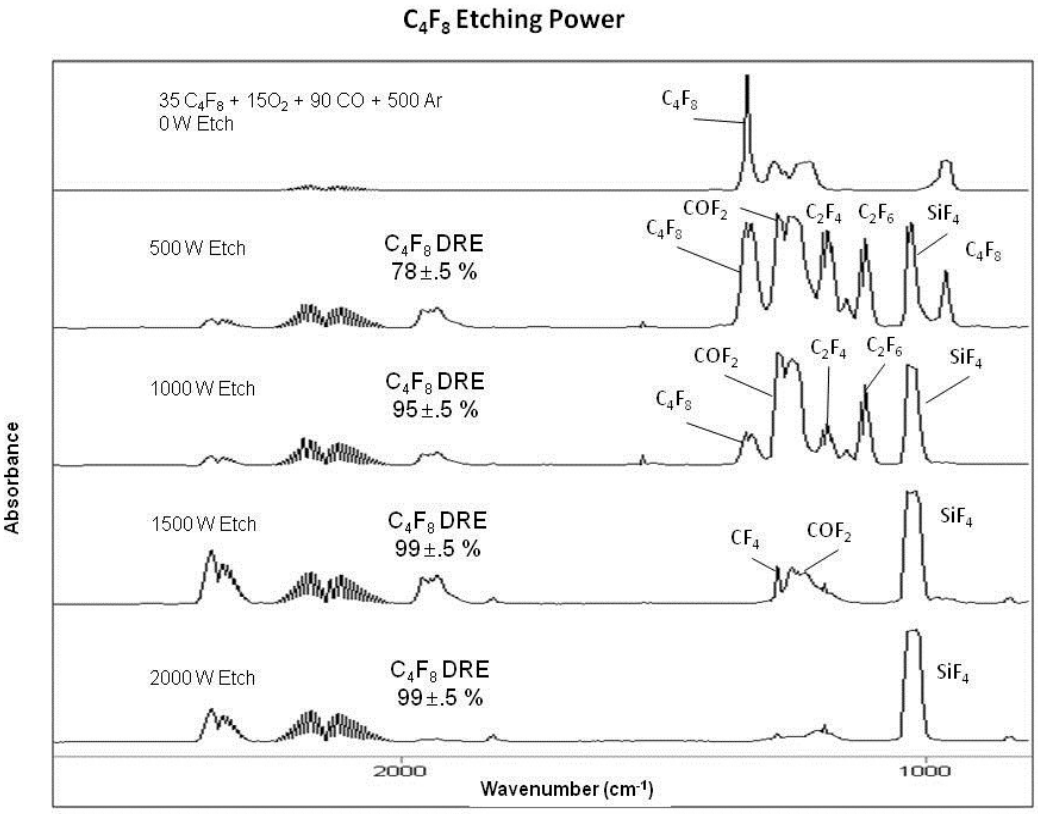


*Figure* 21. $C_4F_8$ Etching of $SiO_2$ Using a Microwave Power Source

### 3.3. Results

Experiments were performed to determine the destruction and removal efficiency (DRE) of the abatement system. The performance can be characterized from the percentage value of the amount of PFC destroyed as shown by the equation,

$$\%DRE = \left( \frac{W_{in} - W_{out}}{W_{out}} \right) x\,100 \quad . \qquad \text{Eq.(29)}$$

$W_{in}$ and $W_{out}$ are the amount of PFCs before and after the abatement reaction. The amount of water was varied using a pressure based flow controller. This allowed for a precise determination of water input and a maximum DRE.

The experiment consisted of process gases only, followed by a 1000 W plasma etching and then a 2000 W abatement. The process gas flow rates (in sccm) were C4F8=35, $O_2$=15, CO=90 and Ar=500. During the abatement the amount of water was varied to determine the maximum DRE. The process steps are shown in Table 7.

Table 7. Experiment Flow and Test Conditions

| | Process Gases | Etch System | Abatement System | Water Added |
|---|---|---|---|---|
| Step 1 | On | Off | Off | Off |
| Step 2 | On | On | Off | Off |
| Step 3 | On | On | On | Off |
| Step 4 | On | On | On | On |

Table 8 shows the experiment matrix: (1) the etching power, (2) the abatement power, (3) the amount of $H_2O$ vapor added, and (4) the resulting DRE. The amount of $H_2O$ vapor was varied for each power level to ascertain the maximum DRE. This data showed that the highest DRE produced was at 80 sccm of $H_2O$ vapor at each level. It also showed that the DRE increased at 500W and 1000W, but was almost the same at 1500W and 1950W. The DRE was calculated using the same method previously described.

Table 8. $C_4F_8$ Etching and Abatement Experiment

| Etch Power[a] (W) | Abatement Power[a] (W) | $H_2O$[b] Added (sccm) | DRE (%) |
|---|---|---|---|
| 1,000 | 0 | 0 | 68.70 ±.05% |
| 1,000 | 500 | 80 | 99.21 ±.05% |
| 1,000 | 1,000 | 80 | 99.97 ±.05% |
| 1,000 | 1,500 | 90 | 99.97 ±.05% |
| 1,000 | 1,950 | 80 | 99.98 ±.05% |
| a Microwave stability ± 0.1%<br>b Flow rate measurements are ± 1% of full scale | | | |

The FTIR results of the experiment are shown in *Figure 22*. The FTIR detected the reactant gases (shown with top line). The middle line shows the gases produced from the plasma "etching" and $SiO_2$ products. The abatement reaction is shown on the bottom line. The major gases produced are HF, CO, $CO_2$ and $SiF_4$. The removal amount $C_4F_8$ calculates to a 99.98 ±.05% DRE.

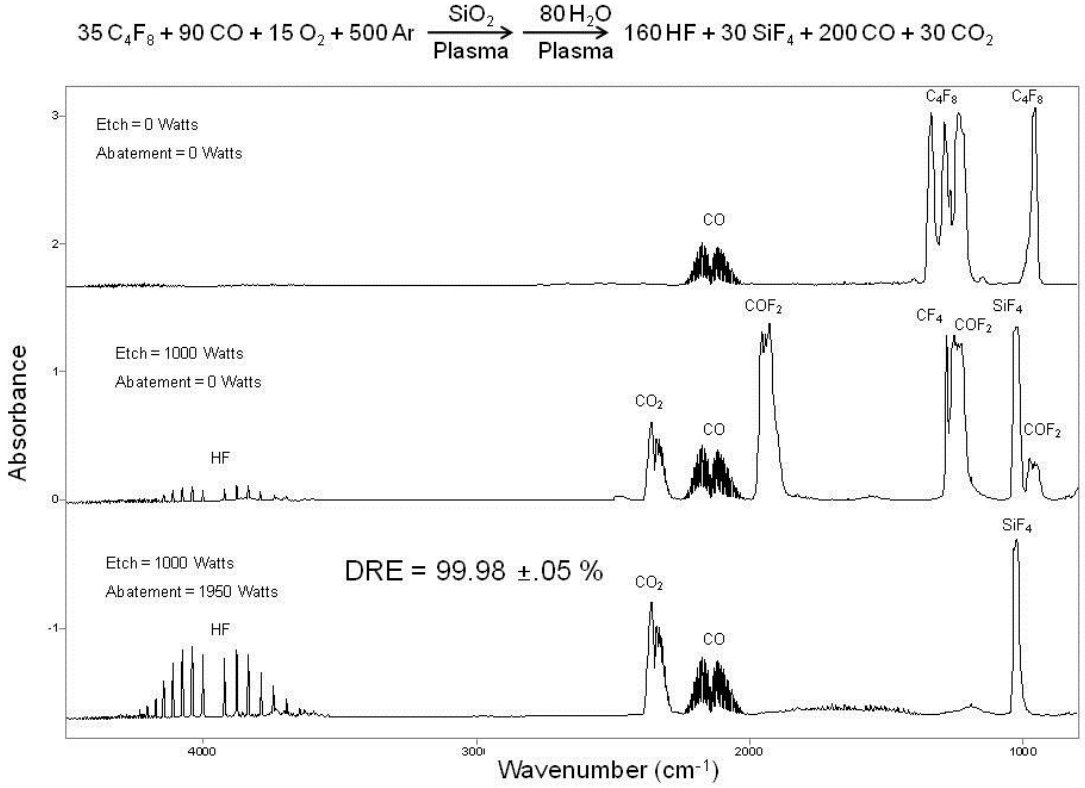


*Figure* 22. FTIR Illustration of $C_4F_8$ Etching and Abatement Byproducts

A mass balanced equation was determined from those results. The idealized stoichiometric equation is given below in Eq.(29).

$$35\ c\text{-}C_4F_8 + 15\ O_2 + 90\ CO + 500\ Ar + 30\ SiO_2 + 80\ H_2O \rightarrow 160\ HF + 30\ SiF_4 + 200\ CO + 30\ CO_2 + 500\ Ar \quad \text{Eq.(29)}$$

The quantitative FTIR analysis is shown in Table 9, where a 97% mass recovery was achieved.

Table 9. $C_4F_8$ Abatement Product Gases

| Microwave Power | Reactor Pressure | DRE | $C_4F_8$ | HF | CO | $CO_2$ | $SiF_4$ | $H_2O$ | Recovery |
|---|---|---|---|---|---|---|---|---|---|
| (W) | (mTorr) | (%) | (ppm) | (ppm) | (ppm) | (ppm) | (ppm) | (ppm) | (%) |
| 1950 | 673 | 99.98 | 0.2 | 3399 | 4358 | 375 | 327 | 89 | 97 |

This methodology was limited because homonuclear diatomic species do not exhibit an induced dipole moment upon infrared excitation and are not observable by FTIR. However, QMS provided complementary qualitative analysis data to the FTIR and was especially useful in identifying molecular and atomic fluorine. Distinctive patterns of mass to charge ratio (m/z) were seen for the reactant gases of c- $C_4F_8$ (200 $C_4F_8^+$: 131 $C_3F_5^+$: 100 $C_2F_4^+$: 69 $CF_3^+$), CO (28$CO^+$: 12$C^+$), Ar (40 $Ar^+$: 20 $Ar^{++}$) and $O_2$ (32 $O_2^+$: 16 $O^+$). Some byproduct fragments that were seen from the etching reaction were $SiF_3^+$, $C_2F_4^+$, $CF_3^+$, $CF_2^+$, $CO^+$, $C^+$, $Ar^+$, $Ar^{++}$, $O_2^+$ and $O^+$. With the 1950W abatement process, the fragments for C:F bonded molecules were abated.

The mass spectra results are shown in *Figure* 23 below. Three peak fragments of $C_4F_8$ are $CF_2^+$ (at m/z 50), $CF_3^+$ (at m/z 69) and $C_2F_4^+$ (at m/z 100). Peak fragments for $CF_4$ include the $CF_3^+$ and $C_2F_4^+$ fragments. The ratio of m/z 50 and m/z 69 peaks indicates the presence of the $CF_4$ molecule in the process stream. The mass spectra and FTIR confirm that $CF_4$ is created during the etching process. During the abatement process the peaks for all fragments disappeared, confirming the destruction of $C_4F_8$.

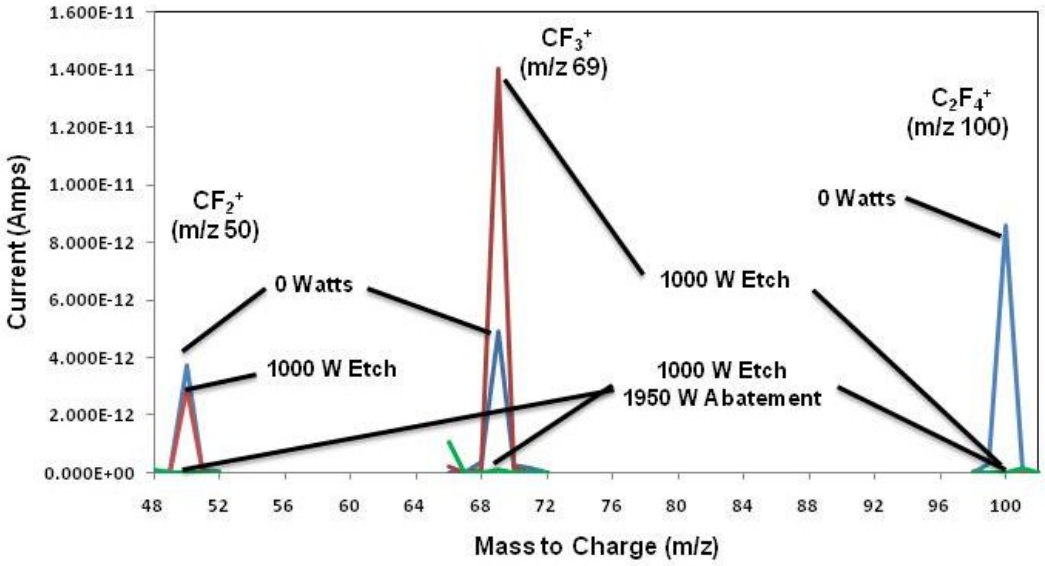


*Figure* 23. Mass Spectra of $CF_2^+$, $CF_3^+$ and $C_2F_4^+$ Peak of $C_4F_8$ Etching and Abatement Byproducts

### 3.4. Discussion

The (PAS) co-developed by R*f* Environmental, Inc. and Texas A&M University has been successful in abating the semiconductor process gas $C_4F_8$ in its un-reacted state. Frantzen showed this with her study of $C_4F_8$ and obtaining results of a 99.93% DRE[1]. Her work showed that the PAS's design produced a plasma column of sufficient density to dissociate the compound of interest. The secondary reactions resulting from the addition of $H_2O$ vapor ensured that the reformation of other GWG compounds did not occur.

This study validates her work by abating $C_4F_8$ after it has reacted with $SiO_2$. Without direct access to the product gases from etching process, a simulated reaction was developed. A simulated etch reaction was created by substituting a radio frequency

power source for a microwave power source. This reaction was critical in producing the compound $SiF_4$. This allowed a second PAS to abate the gases from the etching reaction. The results of showed a DRE of 99.98 ±.05% with a mass recovery of 97%. This showed that addition of the compound $SiF_4$ did not hinder the effectiveness of the PAS in nearly eliminating the most harmful GWGs from the process stream.

# 4. A DETAILED STUDY OF THE ABATEMENT OF POST SILICON OXIDE ($SiO_2$) ETCHING USING CARBON TETRAFLUORIDE ($CF_4$) GAS

## 4.1. Introduction

Experiments have been done to determine the abatement effectiveness of destroying carbon tetrafluoride, $CF_4$ as the reactant gas. A similar experiment was previously performed by Wofford et al at the Motorola semiconductor facility[4]. In their experiments, they abated the product gases from the etch chamber using $H_2$ and $O_2$ additive gases and had a DRE of 99.8%. This study performed a similar experiment using $H_2O$ vapor as the additive gas. The purpose of this study was to simulate radio frequency (≈1-300 MHz) etching plasma using microwave frequency (300MHz – 10 GHz) etching plasma and then abate the waste gases produced ($SiF_4$, CO, $CO_2$, $COF_2$ and $CF_4$) by using another microwave frequency (300MHz – 10 GHz) etching plasma. The hypothesis for the experiments described in this section is that a semiconductor radio frequency etching reaction of $CF_4$ can be simulated using a microwave power source and the products from that reaction can be abated using $H_2O$ vapor as the additive gas to greater than 99% DRE. It will also provide a confirmation of the microwave simulated etching system's ability to replicate the industrial exhaust gases.

A study of the abatement process including the simulated etching process was done similar to previously describe in Chapter III. Thus, the plasma etch reaction is,

$$40\ CF_4 + 15\ O_2 + 160\ Ar + x\ SiO_2 \rightarrow \quad \text{Eq.(30)}$$

$$x\ SiF_4 + a\ CO + b\ CO_2 + c\ COF_2 + d\ CF4 + 160\ Ar.$$

The abatement reaction is then,

$$x\ SiF_4 + a\ CO + b\ CO_2 + c\ COF_2 + d\ CF4 + y\ H_2O \rightarrow \quad \text{Eq.(31)}$$

$$x\ SiF_4 + e\ CO + f\ CO_2 + g\ HF + h\ COF_2.$$

**4.2. Experimental**

The simulated manufacturing recipe is given in standard cubic centimeters per minute (sccm) of each process gas. The experimental equipment and apparatus were the same described in the previous sections (*Figure* 9 and *Figure* 20). The methodology for determining the $CF_4$ etch power was similar to what was described in the previous section for $C_4F_8$. The calibration curve for $CF_4$ is shown in Appendix B.

The amount of $CF_4$ produced has been documented for various combinations of reactants to increase during the etching process[52]. Because of this it is necessary to abate only the waste gases and not just the reactant gases. The following figure (*Figure* 24) shows IR spectra for several etching power levels. The percentage increase of this product has been shown to be as much as 300% for an oxide etch process and 8% for a via etch process[52]. A power level of 500 W produced an increase of 26% in $CF_4$ and was selected for the microwave etching power because it fell between the two published values.

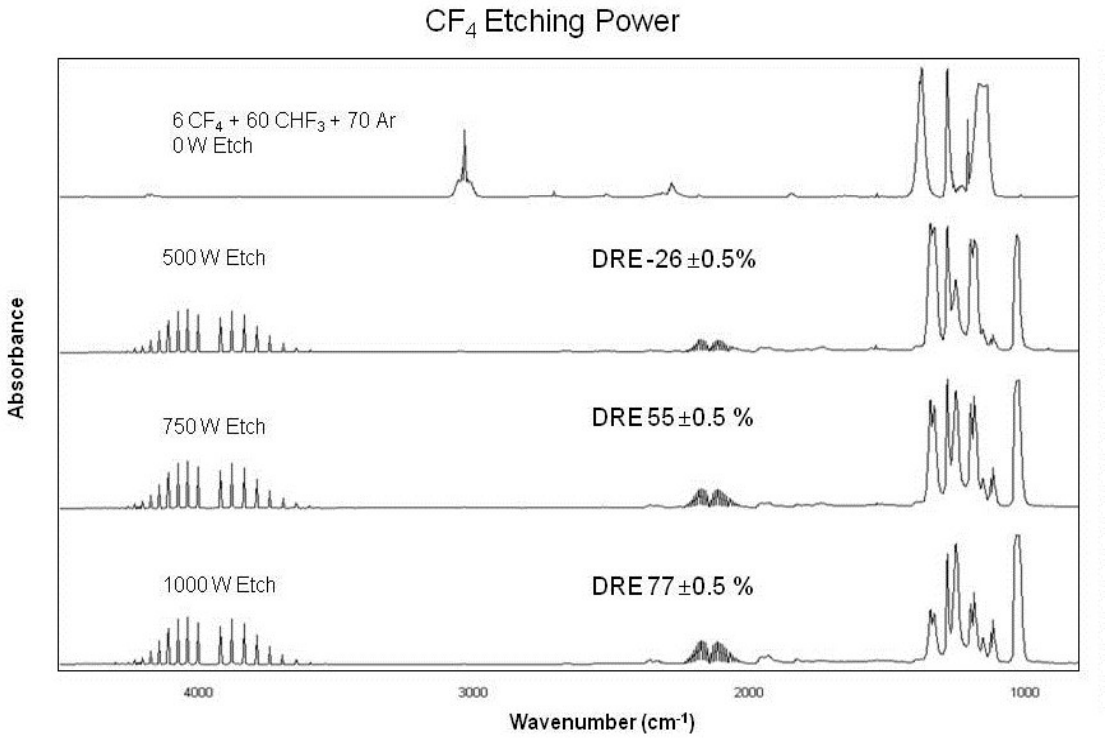


*Figure* 24. $CF_4$ Etching of $SiO_2$ Using a Microwave Power Source

### 4.3. Results

Table 10 shows the experiment matrix: (1) the etching power, (2) the abatement power, (3) the amount of $H_2O$ vapor added, and (4) the resulting DRE. The amount of $H_2O$ vapor was varied for each power level to ascertain the maximum DRE. This data showed that the highest DRE produced was at 50 sccm of $H_2O$ vapor at 1000W. It also showed that the DRE was the same for both $H_2O$ vapor flow rates at 1500W and 2000W.

Table 10. $CF_4$ Etching and Abatement Expermiment

| Etch Power (W)[a] | Abatement Power (W)[a] | H2O (sccm)[b] | DRE[c] (%) |
|---|---|---|---|
| 500 | 0 | 0 | more than -200% |
| 500 | 1,000 | 100 | 99.2 ± .05% |
| 500 | 1,500 | 80 | 99.92 ± .05% |
| 500 | 1,950 | 80 | 99.96 ± .05% |

a Microwave stability ± 0.1%
b Flow rate measurements are ± 1% of full scale
c DRE calculation ± 0.03%

A mass balanced equation was determined from those results. The idealized stoichiometric equation is given below in Eq.(32).

$$40\ CF_4 + 15\ O_2 + 160\ Ar + 80\ H_2O + SiO_2 \rightarrow 40\ SiF_4 + 160\ HF + 70\ CO + 10\ CO_2 + 160\ Ar \qquad \text{Eq.(32)}$$

The results from Table 10 are shown in *Figure 25*. The FTIR detected the reactant gases (shown with top line). The middle line shows the gases produced from the plasma "etching" and $SiO_2$ products. The abatement reaction is shown on the bottom line. The major gases that were produced were HF, CO, $CO_2$ and $SiF_4$. The removal amount $CF_4$ calculates to a 99.96 ±.05% DRE.

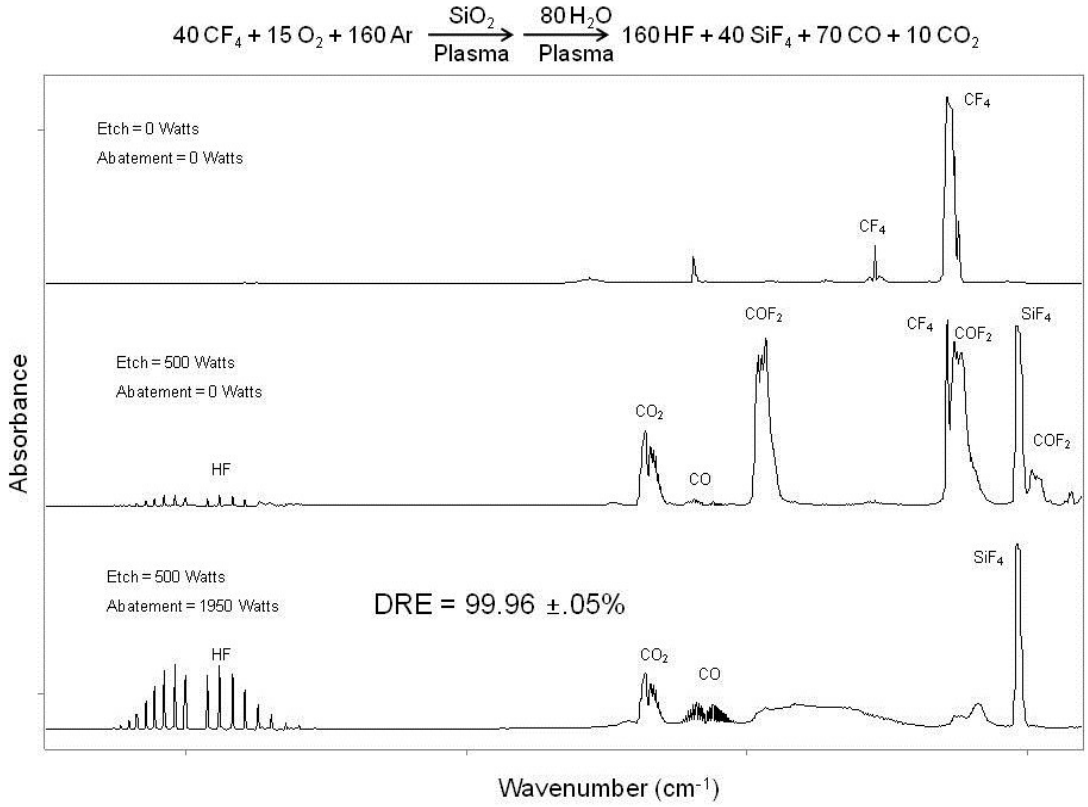


*Figure* 25. FTIR Illustration of $CF_4$ Etching and Abatement Byproducts

The quantitative FTIR analysis is shown in Table 11, where a 95% mass recovery was achieved.

Table 11. $CF_4$ Abatement Product Gases

| Microwave Power | Reactor Pressure | DRE | $CF_4$ | HF | CO | $CO_2$ | $SiF_4$ | $H_2O$ | Recovery |
|---|---|---|---|---|---|---|---|---|---|
| (W) | (mTorr) | (%) | (ppm) | (ppm) | (ppm) | (ppm) | (ppm) | (ppm) | (%) |
| 1950 | 673 | 99.96 | 0.25 | 6110 | 1217 | 127 | 1829 | 129 | 95 |

Distinctive patterns of mass to charge ratio (m/z) were seen for the reactant gases of $CF_4$ (88 $CF_4^+$: 69 $CF_3^+$: 50 $CF_2^+$: 31 $CF^+$: 19 $F^+$), CO (28$CO^+$: 12$C^+$), Ar (40 $Ar^+$: 20

$Ar^{++}$) and $O_2$ (32 $O_2^+$: 16 $O^+$). Some byproduct fragments that were seen from the etching reaction were $SiF_3^+$, $SiO_2^+$, $CF_3^+$, $CO^+$, $C^+$, $Ar^+$, $Ar^{++}$, $O_2^+$ and $O^+$. With the 1950W abatement process, the fragments for C:F bonded molecules were abated.

The following figure (*Figure* 26) shows the mass spectrometer results from the experiment. A peak fragment of $CF_4$ was $CF_3^+$ (at m/z 69). The mass spectra and FTIR confirm that $CF_3^+$, a fragment of $CF_4$ is created during the etching process. During the abatement process the peak for the fragment disappeared, confirming the FTIR results.

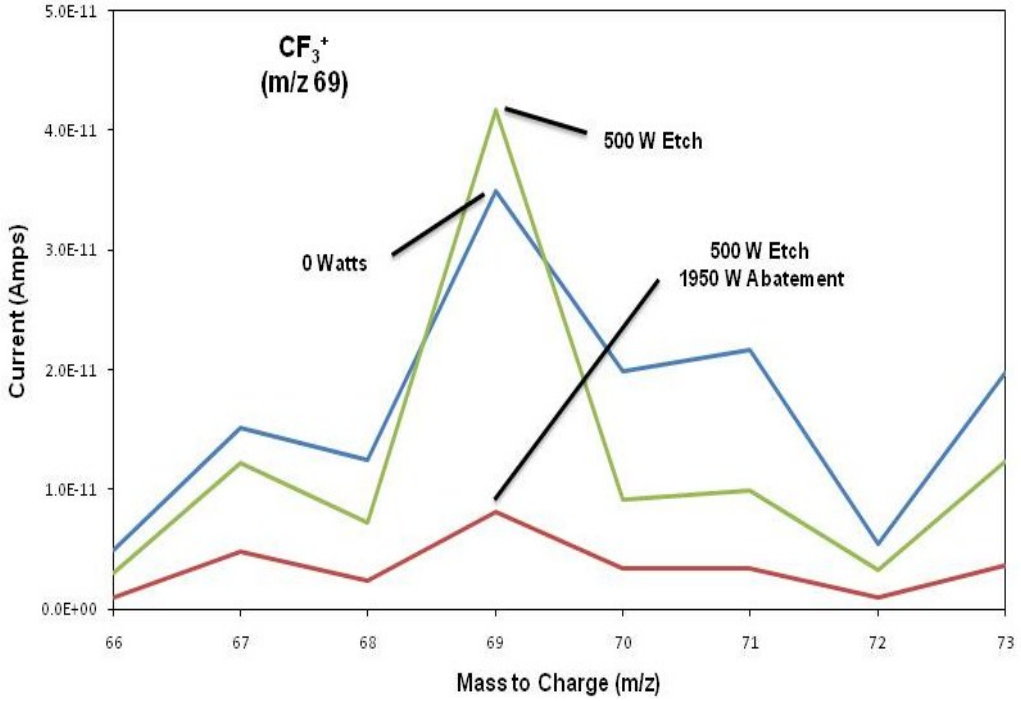


*Figure* 26. Mass Spectra of $CF_3^+$ Peak Resulting from Different Applied Microwave Powers

### 4.4. Discussion

The (PAS) has been successful in abating the semiconductor process gas $CF_4$ [36]. Wofford and Jackson's study of the system showed a DRE for $CF_4$ of 99.8%[36]. Their recipe included the use of $O_2$ and $H_2$ as additive gases. The performance of the system using water vapor gas was slightly lower at 99.96 ±.05% (with a mass recovery of 95%) compared to using pure hydrogen and oxygen.

In retrospect, the calculated DRE showed that the optimal level of $H_2O$ vapor may be less than 80 sccm. Although a wider range of $H_2O$ vapor levels could be used to increase the DRE further, it was again a good confirmation that the previous method was accurate in determining the abatement system's ability to destroy the intended gases.

# 5. CONCLUSION

The 3rd generation plasma abatement system (PAS) co-developed by R*f* Environmental, Inc, and Texas A&M University has been effective at destroying the global warming gases $CF_4$ and $C_4F_8$ [1, 2]. The effectiveness of this system is determined by its ability to abate these particular gases while operating at a low operational cost per unit. The DRE for the system in previous studies has been quantified at 99.8% for $C_4F_8$ by Frantzen[1] and 99.998% for $CF_4$ by Wofford[2]. The cost of ownership rendered the system a viable option for the industrial market with the exception of the cooling system. The previous cooling system used an air cooling design which cost approximately $1400/unit annually. This study's purpose was to modify the cooling system and replicate initial recipe abatement experiments to show the same DRE levels could be attained while reducing operating costs.

A thermodynamic analysis showed a heat flow rate of rate ($\dot{Q}$) was 683W for a 425 lpm air flow cooling design and 723W for a re-circulating liquid cooling design. This substitution allowed for equal heat transfer performance with a greatly improved COO. Based on this research the liquid cooling design was the optimal choice to use given the goals of the abatement system. A conceptual marketing goal was the overall packaging of the system. The design of the packaging was determined by the cost of each fixed unit. Total estimated costs were approximately $20,000. The final sales price is to be determined in the future based upon labor, overhead and a standard mark up percentage.

The design of each experiment was replicated from a combination of previous studies done by Wofford[2-4], Hartz[53], and Frantzen[1] to ensure the abatement procedures were consistent. The purpose of the replication is to make certain of the reliability of the system in a commercial operating setting. Moreover, experimentation with the use of semiconductor process gases and a $SiF_4$ component was needed to determine what would happen in the semiconductor facility. Similar studies for $C_4F_8$ showed an abatement DRE of 99.3%[54] and 99.8%[1]. Studies for $CF_4$ were much more common, and examined using a variety of abatement technologies. These include thermal combustors, tandem packed beds, dielectric barrier discharges, and inductively coupled plasmas with DRE's of 92.5%[54], 59%[55], 95%[56] and 97%[57] respectively. In particular, hydrogen and oxygen concentrations as well as power levels were the main variables for abatement performance. The significance of the abatement process is to reduce the harmful compounds into easily cleaned, low molecular weight compounds CO, $CO_2$ and HF.

The hypothesis in Chapter II that eliminating the forced air convection of the cooling system can maintain system integrity and to reduce the cost of ownership by 50% per year was confirmed. It used forced air convection which operated at a high cost of ownership. The design was modified to replace the air cooling design with a liquid cooling design. The use of an air system was cost prohibitive because the conditioning needed to produce CDA (clean dry air) had a large cost of ownership. The cost of filtering and drying the air at a rate of 425 lpm per unit was $1400. The goal of the

design was to reduce the amount of the air used or use a different medium that would produce the same amount of heat transfer.

Tests to reduce the amount of air used in the cooling system were performed. Vent holes in the outer shell were installed and the flow rate was lowered to less than 142 lpm. Short term testing looked promising, but long term tests resulted in fracturing of the ceramic tube. It was then realized that the temperature differential over the length of the tube was shortening the life of tube. A need for a consistent temperature distribution along the length of the tube was recognized. A liquid cooling design, similar to an automotive radiator was developed. Selection of the Galden HT200 fluid with dielectric constant of less than 9.8 was necessary for the microwaves not to excite the molecules in the fluid and heat it. A feasible product was selected that met the design criteria. Thus, the liquid cooling system design allows for a greater commercial viability while maintaining the correct heat transfer.

The experiment was set up to design and test the temperature of the coolant as it relates to the system's heat dissipation capability. Specifically, did the dielectric fluid remove heat from the surface of the ceramic tube, maintain a constant temperature and dissipate that heat in the plate heat exchanger? In addition, the ability for the PAS to abate CFC gases had to be maintained. During the experiment the chilled water maintained an adequate heat transfer because the temperature of the coolant rose from an initial temperature of 17°C to 43°C. The temperature remained relatively constant for 45 minutes. The results of the coolant being at 40°C was; 1) heat transfer from the ceramic tube and the coolant was taking place, 2) the heat exchanger was removing the heat

energy from the system. The only negative element of the experiment was the Neslab CFT-75 chiller was having difficulty maintaining the set temperature. It had a cooling capacity of 2.5 kW and the microwave generator operated at 2 kW. Considering losses in the heat transfer process, the chiller was slightly undersized for this experiment.

A $C_4F_8$ abatement experiment was run on the liquid cooling design to replicate the results done by Frantzen on an air cooled system. The results from this were 43 ppm of $C_4F_8$, 1.5 ppm of $CF_4$, 113 ppm of $COF_2$ as well as amounts of HF, CO and $CO_2$. This was the most significant negative result for the liquid cooling design. Degradation in the DRE of $C_4F_8$ from 99.98% to 97.5% was disappointing, and $CF_4$ and $COF_2$ were produced as well. The development of a liquid cooling system was then only partially successful. A lower operational cost unit was developed, but the operational performance was less. The efficiency was probably affected by adding another dielectric material in the microwave field, resulting in a less efficient microwave coupling interaction. Further study should be able to resolve this issue.

The second hypothesis, that a semiconductor radio frequency etching reaction of $C_4F_8$ can be simulated using a microwave power source and the products from that reaction can be abated to greater than 99% DRE was confirmed.

A previous study showed the use of $C_4F_8$ showing a 99.8% DRE success rate[1]. The significance of that study proved the abatement process was successful for $C_4F_8$ gas. The production of $SiF_4$ for this experiment was to have a more accurate representation of commercial conditions. The goals of the experiment were to recreate the commercial conditions and successfully abate the exhaust gases. The outcomes of this experiment

include a simulation of the radio frequency etching reaction and the abatement of those exhaust gases. Specifically, the etching process produced $SiF_4$, $COF_2$, $CF_4$ $C_2F_4$ and $C_2F_6$ to mention a few. This provided a closer representation of commercial conditions. The abatement process resulted in a 99.98 ±.05% DRE for $C_4F_8$ with no formation of any other CFC gases.

The third hypothesis that a semiconductor radio frequency etching reaction of $CF_4$ can be simulated using a microwave power source and the products from that reaction can be abated using $H_2O$ vapor as the additive gas to greater than 99% DRE was also confirmed. The previous study abating this gas was done using $H_2$ and $O_2$ gases and achieved a DRE of 99.8 ±.05%[4]. The significance of that study proved the abatement process was successful for $CF_4$ gas. The outcomes of this experiment include a simulation of the radio frequency etching reaction and the abatement of those exhaust gases. The etching process produced similar products as mentioned earlier. The abatement process resulted in a 99.96 ±.05% DRE for $CF_4$ with no formation of any other CFC gases.

The primary CFC gases used by the semiconductor industry for etching are $CHF_3$, $CF_4$, $C_4F_8$, and $C_2F_6$. These do not include all the green house gases used, but they have the longest lifetimes and largest global warming potentials (as shown in Table 2). This plasma abatement system has investigated the destruction of all of these gases to greater than 99% [1-4, 53]. Combining these results with the low cost of ownership, the feasibility of impacting global warming pollution by the semiconductor industry will make this system viable for commercial use. Based on the latest published results the

amount of PFC emissions from the semiconductor industry was 3.6 Tg $CO_2$ Eq. and the total emissions from CFCs, PFCs and $SF_6$ were 4.7 Tg $CO_2$ Eq. [58]. The use of this or a similar abatement technology would have a significant impact on reducing this environmental pollution.

## REFERENCES

[1] M.G. Frantzen, Abatement of perfluorocompounds and chlorofluorocarbons using surface wave plasma technology, Ph. D. Dissertation, Chemistry, Texas A&M University, College Station, TX, 2005.

[2] B. Wofford, J. Bevan, Current status of surface wave plasma abatement of semiconductor global warming emissions, Future Fab International, 11 (2001) 89-95.

[3] B. Wofford, J. Bevan, M. Jackson, Process device for destruction of halocarbons, US Patent, Patent #5,750,823, 1998.

[4] B. Wofford, M. Jackson, C. Hartz, J. Bevan, Surface wave plasma abatement of $CHF_3$ and $CF_4$ containing semiconductor process emissions, Environmental Science and Technology, 33 (1999) 1892-1897.

[5] IPCC, Climate Change 2007: Synthesis Report. Contribution of working groups I, II and III to the fourth assessment report of the Intergovernmental Panel on Climate Change, P. [Core Writing Team, R.K. and Reisnger, A.] (Ed.), IPCC, Geneva, Switzerland, 2007.

[6] U.S. Environmental Protection Agency, Greenhouse gases and global warming potential values: Excerpt from the inventory of U.S. greenhouse emissions and sinks: 1990-2000, U.S. Environmental Protection Agency, Office of Atmospheric Programs, 2002.

[7] H. Le Treut, R. Somerville, U. Cubasch, Y. Ding, C. Mauritzen, A. Mokssit, T. Peterson and M. Prather, Historical overview of climate change. In: Climate Change 2007: The physical science basis. Contribution of working group I to the fourth assessment report of the intergovernmental panel on climate change, S. Solomon, D. Qin, M. Manning, Z. Chen, M. Marquis, K.B. Averyt, M. Tignor, H.L. Miller (Eds.), Cambridge University Press, Cambridge, United Kingdom and New York, NY, USA, 2007.

[8] U.S. Environmental Protection Agency, Inventory of U.S. greenhouse gas emissions and sinks 1990-2007 EPA, 2009.

[9] K.E. Trenberth, P.D. Jones, P. Ambenje, D.E. R. Bojariu, A. Klein Tank, D. Parker, F. Rahimzadeh, J.A. Renwick, M. Rusticucci, B. Soden, P. Zhai, Observations: Surface and Atmospheric Climate Change, S. Solomon, D. Qin, M. Manning, Z. Chen, M. Marquis, K.B. Averyt, M. Tignor, H.L. Miller (Eds.) Climate Change 2007: The Physical Science Basis, IPCC, Cambridge, United Kingdom and New York, NY, USA, 2007.

[10] World Semiconductor Council, Joint statement of the 12th meeting of the World Semiconductor Council (WSC), Taipei, China, 2008, pp. 20.

[11] Joint Steering Committee (JSTC) of the World Semiconductor Council (WSC), JSTC statement on the green house gas legislation, 2005.

[12] Semiconductor Industry Association (SIA) position paper: "Setting an international PFC emissions reduction goal for the semiconductor industry", 1999.

[13] S. Bartos, D. Lieberman, S. Burton, Estimating the impact of migration to Asian foundry production on attaining the WSC 2010 PFC reduction goal, International Semiconductor Environment, Safety and Health (ISESH) Conference, EPA, Makuhari, Japan, 2004.

[14] M.B. Chang, Abatement of PFCs from semiconductor manufacturing processes by nonthermal plasma technologies: A critical review, Industrial & Engineering Chemistry Research, 45 (2006) 4101-4109.

[15] T. Streif, G. DePinto, S. Dunnigan, A. Atherton, PFC reduction through process and hardware optimization, Semiconductor International, 20 (1997) 129-132.

[16] U.S. Environmental Protection Agency, U.S. high GWP gas emissions 1990–2010: Projections, and opportunities for reductions June 2001, U.S. Environmental Protection Agency (Ed.), Washington, DC, 2001.

[17] L. Beu, P.T. Brown, Motorola's strategy for reducing PFC emissions, IEEE/CPMT International Electronics Manufacturing Technology Symposium, 1998, pp. 277-285.

[18] W.T. Tsai, H.P. Chen, W.Y. Hsien, A review of uses, environmental hazards and recovery/recycle technologies of perfluorocarbons (PFCs) emissions from the semiconductor manufacturing processes, Journal of Loss Prevention, 15 (2002) 65-76.

[19] B. Cummins, T. Gilliland, M. Richards, K. Trilli, S. Kesari, Evaluation of Air Liquide's perfluorocompound (PFC) capture technology (ESHC002), 7013229A-TR, International SEMATECH 1997.

[20] W. Worth, Reducing PFC emissions: A technology update, Future Fab International, 9 (2000).

[21] E.J. Tonnis, V. Vartanian, L. Beu, T. Lii, R. Jewett, D. Graves, Evaluation of a Litmas "Blue" point-of-Use (POU) plasma abatement device for perfluorocompound (PFC) destruction, 98123605A-ENG, International SEMATECH, 1998.

[22] V. Vartanian, L. Beu, T. Lii, D. Graves, E. Tonnis, R. Jewett, B. Wofford, J. Bevan, C. Hartz, M. Gunn, Plasma abatement reduces PFC emission, Semiconductor International, 23 (2000) 191-196.

[23] M. Radoiu, Studies on atmospheric plasma abatement of PFCs, Radiation Physicis and Chemistry, 69 (2004) 113-120.

[24] K. Suzuki, Y. Ishihara, K. Sakoda, Y. Shirai, A. Teramoto, M. Hirayama, T. Ohmi, T. Watanabe, T. Ito, High-efficiency PFC abatement system utilizing plasma decomposition and $Ca(OH)_2$/CaO immobilization, IEEE Transactions On Semiconductor Manufacturing, 21 (2008).

[25] Semiconductor Industry Association (SIA), About SIA: Driving progress and results, Semiconductor Industry Association, San Jose.

[26] U.S. Environmental Protection Agency, Inventory of U.S. greenhouse gas emissions and sinks: 1990 - 2004, 2006.

[27] P. Forster, V. Ramaswamy, P. Artaxo, T. Berntsen, R. Betts, D.W. Fahey, J. Haywood, J. Lean, D.C. Lowe, G. Myhre, J. Nganga, R. Prinn, G. Raga, M. Schulz, R.V. Dorland, Changes in atmospheric constituents and in radiative forcing. In: Climate Change 2007: The physical science basis. Contribution of working group I to the fourth assessment report of the Intergovernmental Panel on Climate Change, S. Solomon, D. Qin, M. Manning, Z. Chen, M. Marquis, K.B. Averyt, H.L.M. M. Tignor (Eds.), Cambridge University Press, Cambridge, United Kingdom and New York, NY, USA, 2007.

[28] J. Williams, PFC emissions reduction: Technical requirements and challenges for semiconductor operations, Semiconductor Fabtech, 2005, pp. 73-80.

[29] Reduction of perfluorocompound (PFC) emissions: 2005 State-of-the-Technology Report, International SEMATECH Manufacturing Initiative, 2005.

[30] T. Ohiwa, I. Sakai, K. Okumura, A new gas circulation RIE, IEEE Transactions on Semiconductor Manufacturing, 13 (2000) 310-314.

[31] H. Xie, Abatement of perfluorocompounds with microwave plasma in atmospheric pressure environment, Journal of Hazardous Materials, 168 (2009) 5.

[32] R. Brown, J. Rossin, C. Thomas, Catalytic process for control of PFC emissions, Semiconductor International, June 2001.

[33] T. Walling, A. Tran, B. Ridgeway, Evaluation of an Edwards TPU4214 and an Ecosys Phoenix IV for CF4 Abatement (ESHC002), SEMATECH, International, 1997.

[34] J. Arno, J. Bevan, M. Moisan, Acetone conversion in a low-pressure oxygen surface wave plasma, Environmental Science and Technology, 29 (1995) 1961-1965.

[35] J. Arno, J. Bevan, M. Moisan, Detoxification of trichloroethylene in a low-pressure surface wave plasma reactor, Environmental Science and Technology, 30 (1996) 2427-2431.

[36] V. Vartanian, L. Beu, T. Lii, B. Wofford, C. Hartz, J. Bevan, Evaluation of R*f* Environmental Systems/Texas A&M University surface wave plasma device for abatement of perfluorocompound (PFC) emissions (ESHC005), 98093561A-ENG, International SEMATECH, 1998.

[37] B. Derecskei, M. Gunn, J.W. Bevan, B. Wofford, Reduction of semiconductor global warming emission gases using surface wave plasma with water as a source of radicals, Unpublished manuscript, Texas A&M University, College Station, 1999.

[38] L. Beu, Results of the ISMI ESH technology center greenhouse gas facility survey 09065012A-TR International SEMATECH 2009.

[39] M. Moisan, Z. Zakrzewski, Plasma sources based on the propagation of electromagnetic surface-waves, J Phys D Appl Phys, 24 (1991) 1025-1048.

[40] M. Moisan, Z. Zakrzewski, R. Pantel, The theory and characteristics of an efficient surface wave launcher (surfatron) producing long plasma colums, Journal of Applied Physics, 12 (1979) 219-238.

[41] Y. Kabouzi, M. Moisan, J. Rostaing, C. Trassy, D. Guerin, D. Keroack, Z. Zakrzewski, Abatement of perfluorinated compounds using microwave plasmas at atmospheric pressure, Journal of Applied Physics, 93 (2003) 9483-9497.

[42] M. Moisan, J. Peltier, Microwave Excited Plasmas, Elsevier: Amsterdam, 1992.

[43] C.M. Ferreira, M. Moisan, Microwave Discharges: Fundamentals and Applications, Plenum Press, New York, 1993.

[44] P. Van Zant, Microchip Fabrication : A Practical Guide to Semiconductor Processing, 3rd ed., McGraw-Hill, New York, 1997.

[45] H. Conrads, M. Schmidt, Plasma generation and plasma sources, Plasma Sources Science and Technology, 9 (2000) 441-454.

[46] M. Moisan, Z. Zakrzewski, R. Pantel, P. Leprince, Waveguide-based laucher to sustain long plasma coumns through the propagation of an electromagetic surface wave, IEEE Transactions on Plasma Science, PS-12 (1984) 203-214.

[47] D. Lide, CRC Handbook of Chemistry and Physics, CRC Press, Inc, Boca Raton, FL, 1992.

[48] B. Derecskei, R&D result of the 3" OD surface wave plasma abatement device, Unpublished raw data, Texas A&M University, College Station, 2001.

[49] A.F. Mills, Heat Transfer, 2 ed., Prentice Hall, Upper Saddle River, NJ, 1999.

[50] Department of Energy, Compressed air tip sheet #1, DOE/GO-102000-0986, 2000.

[51] M. O'Halloran, Fab utility cost values for cost of ownership (COO) calculations, 02034260A-TR, International SEMATECH, 2002.

[52] W. Worth, Tool perfluorocompound (PFC) emissions data report, 96073156B-ENG, SEMATECH International, 1997.

[53] C. Hartz, J. Bevan, M. Jackson, B. Wofford, Innovative surface wave plasma reactor technique for PFC abatement, Environmental Science and Technology, 32 (1998) 682-687.

[54] M. Radoiu, S. Carss, A. Seeley, J.V. Gompel, Sixty percent utilities savings on etch PFC abatement, Semicon West 2003, BOC Edwards, 2003.

[55] H.L. Chen, H.-M. Lee, L.C. Cheng, M.B. Chang, S.J. Yu, S.-N. Li, Influence of nonthermal plasma reactor type on $CF_4$ and $SF_6$ abatements, IEEE Transactions On Plasma Science, 36 (2008).

[56] G.J. Pietsch, A.B. Saveliev, Treatment of carbon tetrafluoride with gas discharges, Plasma Processes and Polymers, 2007 (2007) 6.

[57] R. Jewett, Atmospheric pressure plasma abatement of perfluorinated compounds (PFCs) in industrial exhaust streams, Future Fab International, 12 (2002).

[58] United States Department of State, U.S. climate action report 2010, Global Publishing Services, Washington, 2010.

# APPENDIX A

## SAMPLE CALCULATIONS

1. Determine Calibration Curve for HF
    - Determine ppm range of curve i.e 30 - 8000 ppm
    - Obtain 1% HF(g) balanced in $N_2$(g)
    - Make dilution spreadsheet to calculate ppm at various flow rates
        - Calibration gas concentration ppm * Cal gas flow rate (L)/Total flow rate (L)

$$\frac{9651\ ppm \times 5\ L/min}{35\ L/min} = 1378\ ppm$$

    - Obtain FTIR and MS using the gas at various flow rates
    - Integrate peak areas between 4400-3400 $cm^{-1}$ (asymmetric stretch)
    - Make a graph of peak area vs. ppm
    - Insert a trend line to obtain an equation of the curve.
2. Conversion of Peak Area to ppm for HF
    - Integrate spectra peak area using Bomem Grams 32 software
    - Insert average in calibration curve to obtain ppm
        - $ppm = -0.1469x^3 + 14.424x^2 + 6.8388x$
        - $-0.1469*(22.28)^3 + 14.424*(22.28)^2 + 6.8388*(22.28) = 5687$ ppm
3. Obtain DRE for Experiment
    - Determine pre-plasma ppm of *c*-C4F8
        - Total Flow Rate of Reaction

- ❖ 35 *c*-$C_4F_8$ + 90 CO + 15 $O_2$ + 500 Ar + 30,000 $N_{2\ Purge}$ = 30720 sccm

- $\left(\frac{35}{30720}\right) = 1.139 * 10^{-3} \times 1 * 10^{6} = 1139\ ppm$

- Integrate peak area of *c*-C4F8 between 1370-1175 $cm^{-1}$
- Insert into calibration curve
- Calculate DRE
  - $1 - (\frac{1139-1.43}{1139}) = 99.87$

4. Mass balance the recipe
   - Stoichiometrically balance the reaction
     - 35 *c*-$C_4F_8$ + 90 CO + 15 $O_2$ + 500 Ar + 80 $H_2O$ + 30 $SiO_2 \longrightarrow$ 30 SiF4 + 160 HF + 200 CO + 30 $CO_2$
   - Convert all by-products to ppm from calibration curves
     - HF = 3751 ppm
     - CO = 4775 ppm
     - $CO_2$ = 627 ppm
     - $SiF_4$ = 327 ppm
     - $C_4F_8$ = 0.2 ppm
     - $H_2O$ = 89.4 ppm
   - Determine percentage of total flow
     - HF: $V = \frac{(3751\ ppm)(30720 ml)}{1{,}000{,}000} = 115.23\ ml$
   - Using the ideal gas law convert to moles

- For HF: $n = \frac{PV}{RT} = \frac{(1\ atm)(115.23\ ml)}{(0.0821\ \frac{ml \cdot atm}{K \cdot mol})(361\ K)} = 3.9\ mol$
- Calculate ratio from stoichiometric equation
  - Ratio = 160 / 3.9 = 41
- Sum total of calculated moles
- Sum total of stoichiometric moles
- Calculate percent difference
  - $1 - \left(\frac{420-408}{408}\right) = 97\%$ mass recovery

# APPENDIX B

## CALIBRATION CURVES

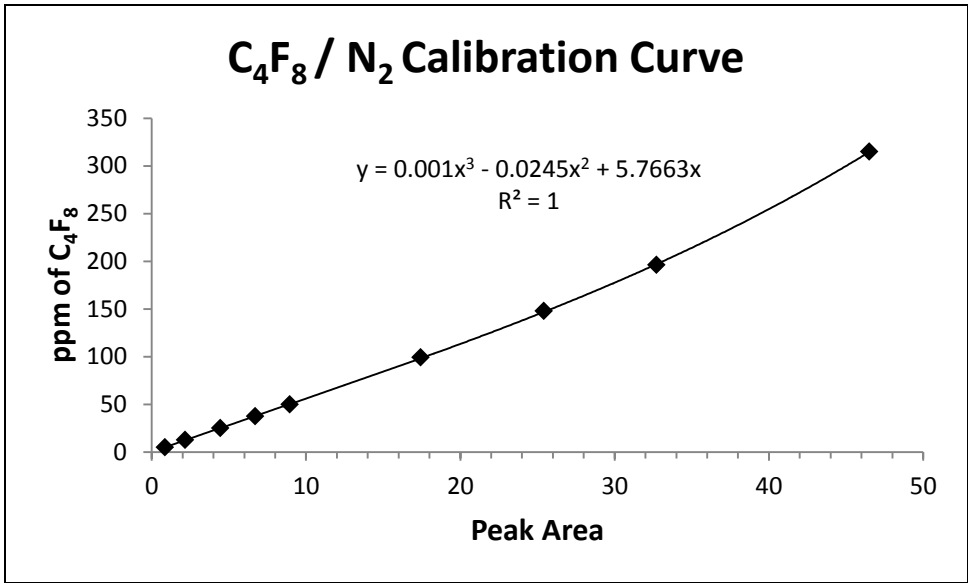


Figure B - 1 Octafluorocyclobutane Calibration Curve

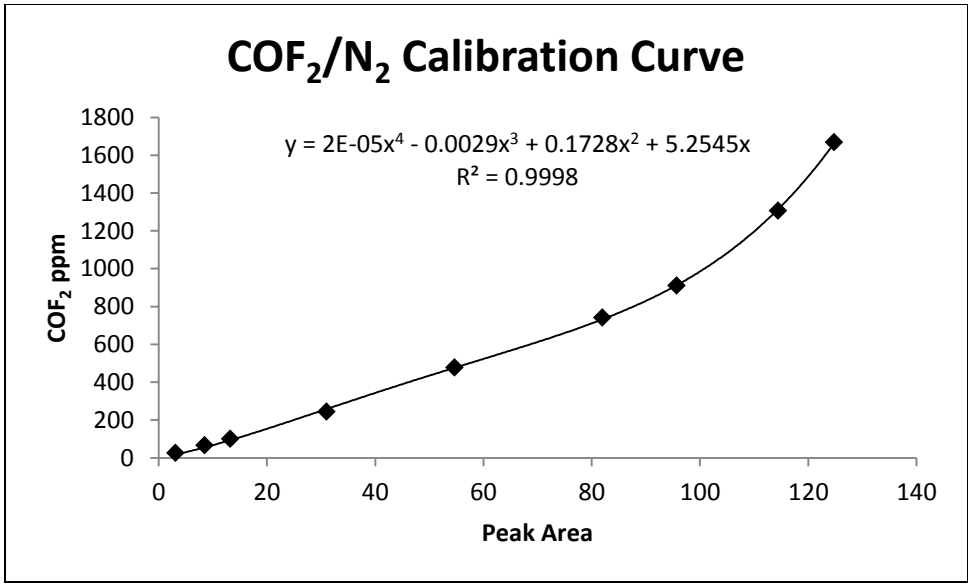


Figure B - 2 Carbonyl Fluoride Calibration Curve

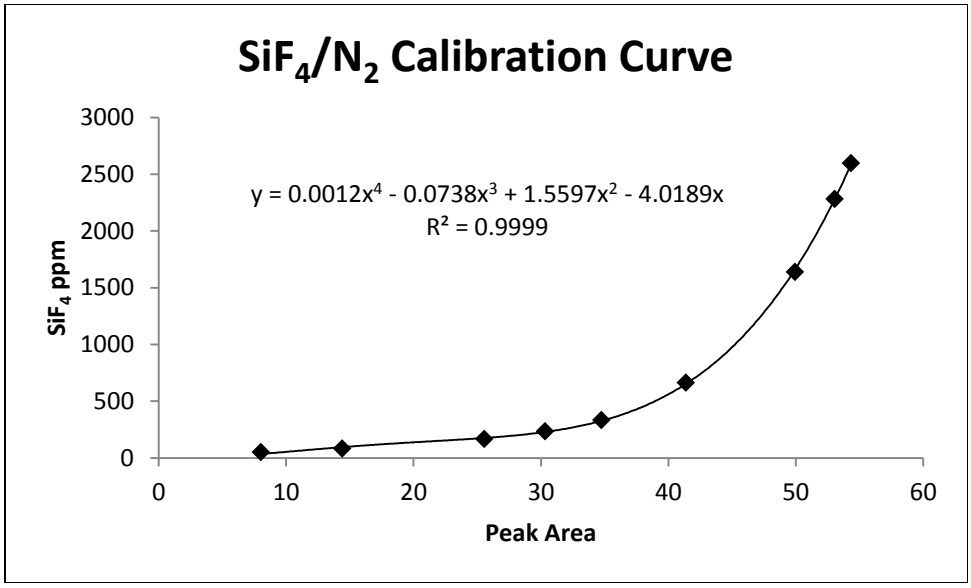


Figure B - 3 Silicon Tetrafluoride Calibration Curve

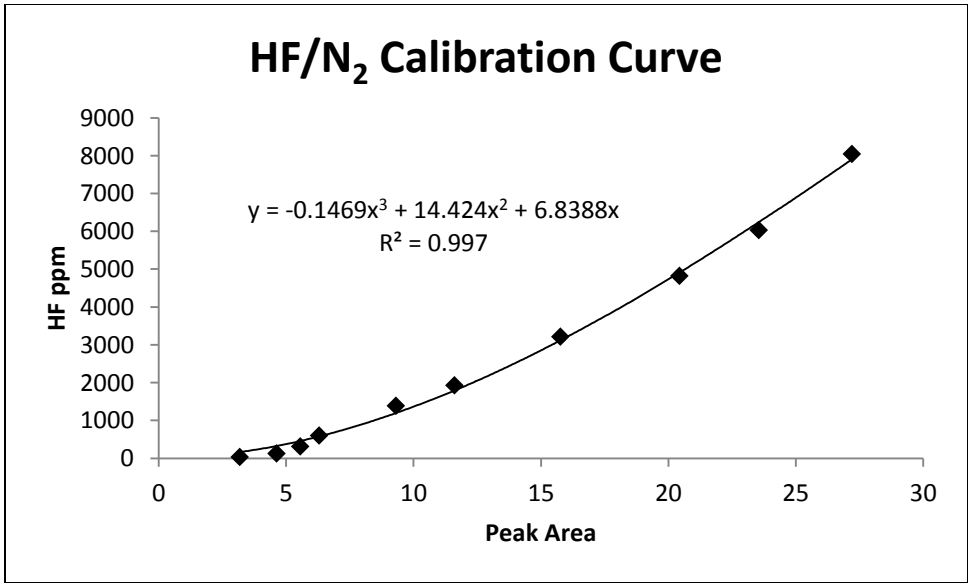


Figure B - 4 Hydrogen Fluoride Calibration Curve

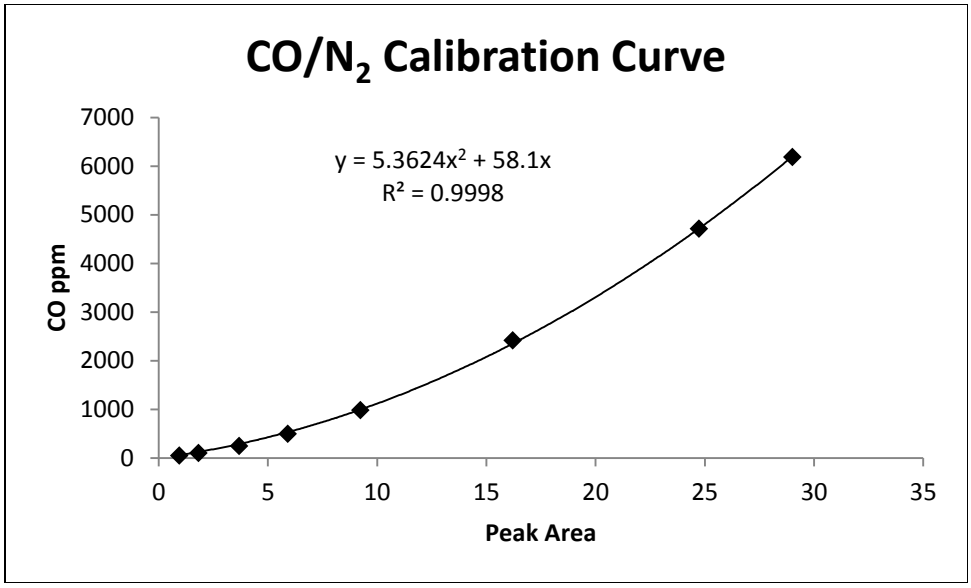


Figure B - 5 Carbon Monoxide Calibration Curve

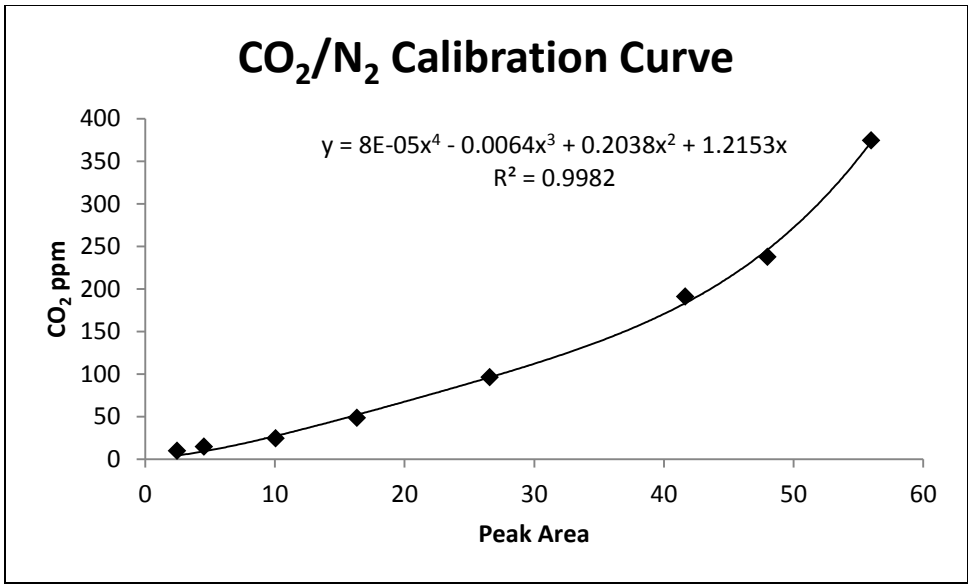


Figure B - 6 Carbon Dioxide Calibration Curve

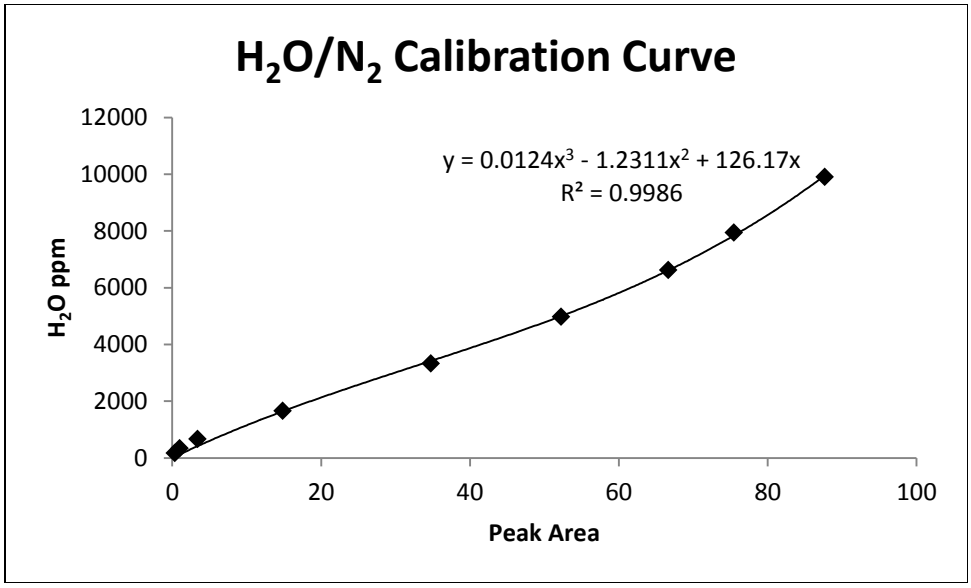


Figure B - 7 Water Vapor Calibration Curve

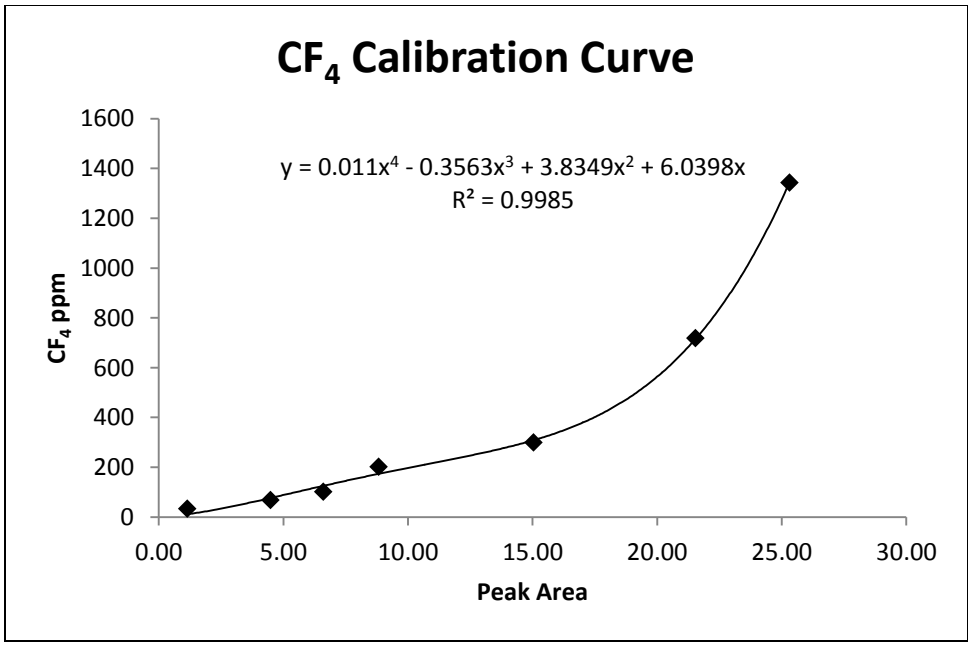


Figure B - 8 Carbon Tetrafluoride Calibration Curve

# VITA


Name: Matthew Robert Butler

Address: Texas A&M University
Department of Mechanical Engineering
3123 TAMU
College Station TX 77843-3123

Email Address: matthewrbutler@yahoo.com


Education: B.S., Mechanical Engineering, New Mexico State University, 1996

M.S., Mechanical Engineering, Texas A&M University, 2011